Hamburg University of Technology

Master Thesis

Study and optimization of the degree of separation of nanofiltration according to operating parameters and molecular structure

Submitted by:

Emmanuel Fuentes Othman-Bentría

Study program: Mechanical Engineering and Management – MEM

Matriculation No: 497226

1st Examiner:	Prof. Dr.-Ing Ralf Otterpohl
2nd Examiner	Dr.-Ing Joachim Behrendt
Supervisors:	Dr.-Ing Joachim Behrendt
	Dr.-Ing Alicia Iborra Clar

Institute of Wastewater Management and Water Protection

Hamburg, 07/07/2021

Statement of Honour

I hereby declare that I personally have completed the present scientific work. The ideas obtained from other direct or indirect sources have been indicated clearly. This work has neither been submitted to any other course or exam authority, nor has previously been published.

Place, Date	Signature

Table of Contents

List of Figures

List of Tables

Abstract

Water pollution is one of the main problems for the human health and for the environment nowadays. This contamination, which has different sources, such as industries, hospitals, households, etc., needs to be erased from the effluents in order to reuse this water for the living beings, as well as for the nature in general.

In this Master Thesis the possibility of erase dyes from the water is studied. The dyes studied are Methylene Blue (MB), Brilliant Green (BG) and Acid Orange 7 (AO7). These dyes are widely used in the textile industry, as well as in other fields such as the pharmacy, plastic, or cosmetic industries.

To eliminate these dyes, a nanofiltration membrane has been used. This wastewater treatment method has several advantages, such as its ability to remove any dye, its high efficiency, and its reasonable overall cost.

In order to evaluate the membrane efficiency in removing these dyes, the influence of the feed pressure or the feed flow has been studied, as well as some parameters like the recovery ratio, which can describe the membrane performance.

The experimental results shows that this method can eliminate in a great way these dyes that have been studied, showing rejection factors around 90% in the case of MB and around 99% in the case of the other two dyes (BG and AO7).

1. Introduction

Water is a vital element for every form of life. From humans to other living beings, it is needed by all. Hundreds of years ago, it was considered as an unlimited renewable resource, but in this century and during the second half of the 20th century it has become evident that this resource is not unlimited anymore, to the extent that water is, since last year, listed on Wall Street stock exchange. Despite that, human beings have been increasingly polluting water, so the scientific community has concentrated his efforts on wastewater treatments to return it to the environment without any danger, given the fact that around 80% of the wastewater without any type of treatments have negative effects in the environment. (Bashanaini, Al-Douh, & Al-Ameri, 2019)

There are some pollutants which are not easily removed from the water stream, so we need special treatments. One of the main sources of pollutants are industries, such as the textile industry which mainly uses one of the worst pollutants: dyes (Khosravi, Karimi, Ebrahimi, & Fallah, 2020). But dyes are not only used in this type of industries, they are also used in leather, food and beverages, paints and medicine industries. (Bhattacharya, et al., 2019). The harmfulness of dyes is due to its high chromaticity, toxicity, carcinogenicity and difficult degradation, which can cause severe issues in the environment. Dyes can also prevent aquatic plants from doing the photosynthesis, as they absorb the visible light in high quantities, causing the disruption in the first steps of the food chain. Moreover, these pollutants can enter in the human body, harming seriously our health. (Bashanaini, Al-Douh, & Al-Ameri, 2019), (Ding, et al., 2020) (Li, et al., 2017).

In order to protect water supplies, authorities have developed a series of more restrictive laws concerning wastewater treatments. It is utterly important to protect natural resources, implementing new techniques to eliminate the pollutants in them, such as dyes.

In efforts to achieve this goal, several physical and chemical methods are used, such as adsorption, biological treatments, advanced chemical oxidation, electrocoagulation, etc. Nevertheless, these methods are not able to fulfil all the requirements that environmental laws now demand for, as avoiding the creation of xenobiotic components or not being able to erase the colour of the wastewater or reduce the high conductivity. One of the methods that accomplish these requirements is membrane nanofiltration, which is also capable of reducing operational costs and water consumption by recycling the water. Furthermore, it has an excellent retention ability of small organic molecules and multivalent ions. (Khosravi, Karimi, Ebrahimi, & Fallah, 2020), (Zuriaga-Agusti, et al., 2010), (Kang, Shao, Chen, Dong, & Qin, 2021).

The type of membrane that has been used in this work has been a polyamide thin-film composite membrane (PA TFC), which is ideal for treating ground and surface water where it is planned to eliminate organic materials with partial softening. (Li, et al., 2021), (DOW)

The dyes to remove from wastewater in this work are Methylene Blue (MB), Brilliant Green (BG) and Acid Orange 7 (AO7). Methylene blue is a cationic dye, easily soluble in water and which has a strong dark blue colour. It was firstly used as a dye in the textile industry, but nowadays is used mainly in the medicine field to treat methemoglobinemia, urinary tract infections, etc. It is also used in chemistry and biology areas. (Thesnaar, Bezuidenhout, Petzer, Petzer, & Cloete, 2021). With regard to brilliant green, this is a triphenylmethane based dye which is mainly used in the textile, biology and medicine fields. (Bhattacharya, et al., 2019), (Khan, et al., 2020). Both dyes can have negative effects while tainting water supplies, causing health issues associated to kidney and lungs (BG) or having a neurotoxic effect on the central nervous system (MB). (Thesnaar, Bezuidenhout, Petzer, Petzer, & Cloete, 2021), (Bhattacharya, et al., 2019), (Khan, et al., 2020). Finally, Acid Orange 7 is an azo dye which broad use in the cosmetic, detergent or paper printing industries. Presents similar negative effects as the other two dyes, like carcinogenicity and toxicity. (Wang, et al., 2021) (Swain, et al., 2021).

Therefore, the aim of this master's Thesis is to investigate the removal of these dyes from wastewater by using nanofiltration, evaluating the capacity of this membrane and its viability to eliminate them in certain conditions. To reach this aim the following studies are proposed:

- Study of feed pressure influence
- Study of feed flow influence
- Study of membrane performance

2. Theoretical background

2.1. Pollution

According to the definition given in the Spanish law (Real Decreto 817/2015), pollution is defined as "the direct or indirect introduction, as a consequence of the human activity, of substances or energy in the atmosphere, water or soil, which can be damaging to human health or to the quality of aquatic ecosystems, or terrestrial ecosystems that depend on aquatic ecosystems, and which cause harm to material goods, damage or complicate the benefits and other legitimate uses of the environment"

As for the water pollution, the definition provided by the OECD is "the presence in water of harmful and objectionable material, obtained from sewers, industrial wastes and rainwater, in sufficient concentrations to make it unfit for use."

The main causes of water pollution are the emission of domestic and urban wastewater, as well as the effluent coming from the industrial and agricultural sectors (Khan, et al., 2020). Nowadays, we can find many kinds of pollutants in the water, like oils, inorganic salts, heavy metals, acids, and dyes. (Wasewar, Singh, & Kansal, 2020)

2.2. Dyes

2.2.1. Definition and history of dyes

A colourant is a substance that is capable of tint the animal and vegetal fibres, changing the colour of them. They can give colour to substances because they have two main groups in their chemical structure: chromophores and auxochromes. Chromophores are the groups that make the molecule absorb light in the visible spectrum of the electromagnetic spectrum, generating the colour. An auxochrome is a functional group that does not impart colour by itself, but if it is conjugated with a chromophore group increases the colour intensity. (Pavithra & Jaikumar, 2019), (Elvers, Hawkins, & Schulz, 2002), (Gupta V. K., 2009).

Colourants are divided in two categories: dyes and pigments. The main differences between them is that while dyes are soluble, have small sizes and are organic molecules pigments are insoluble, bigger (1-2 µm) and inorganic. (Pavithra & Jaikumar, 2019). Dyes are defined by ETAD (The Ecological and Toxicological Association of Dyes and organic pigments) as "intensely coloured or fluorescent organic substances only, which impart colour to a substrate by selective absorption of light".

Despite the use of dyes is known since the Ancient history, the first synthetic dye, the Mauveine, was discovered in 1856 by William Perkin. Since then, and with the arrival of organic chemistry as a new field, thousands of dyes have been synthesized in a short period of time. (Elvers, Hawkins, & Schulz, 2002). Nowadays, synthetic dyes are used in many industries, such as textile, printing, food processing, tanneries, distilleries,

cosmetics, plastics, etc. It is estimated that are around 100.000 commercial dyes with a production of over 7×10^5 tons annually. (Pavithra & Jaikumar, 2019), (Yagub, Sen, Afroze, & Ang, 2014).

2.2.2. Classification of dyes

In order to classify colourants (and therefore dyes), the Society of Dyers and Colourists and the American Association of Textile Chemists and Colourists (AATCC) published in 1925 the Colour Index, an official reference guide with all the basic colourants. It is worldwide recognised and has listed around "27.000 individual products under 13.000 Colour Index™ Generic Names".

This index uses a system which is dual. The most common used descriptor is the CI Generic Name (CIGN), which is related to the application process, and the other descriptor is the CI Constitution Number (CICN), associated with the chemical structure of the dye. By its usage class (recognised by the users), its tone and its serial number (made by the chronological order in which the colourants have been registered in the Colour Index) the CIGN is able to describe a commercial product. (Introduction to the Colour Index: Classification System and Terminology, 2013)

In what refers to dyes, it is possible to classify commercial ones according to their application, chemical structure and their particle charge upon dissolution in aqueous application medium. The classification made according to their chemical structure has many advantages, as it allows to know immediately to which group the dye belongs to and which properties has. Furthermore, is the main system used by the synthetic dye chemist and the dye technologist. (Pavithra & Jaikumar, 2019), (Yagub, Sen, Afroze, & Ang, 2014), (Gupta V. K., 2009).

According to their chemical structure, dyes are classified as it follows:

- Azo dyes
- Anthraquinone dyes
- Indigoid dyes
- Nitroso dyes
- Nitro dyes
- Triarylmethane dyes

In *Figure 2.1* it is given the chromophore of these type of dyes according to their chemical structure. Every dye that belongs to a certain type of dye has this chromophore in common.

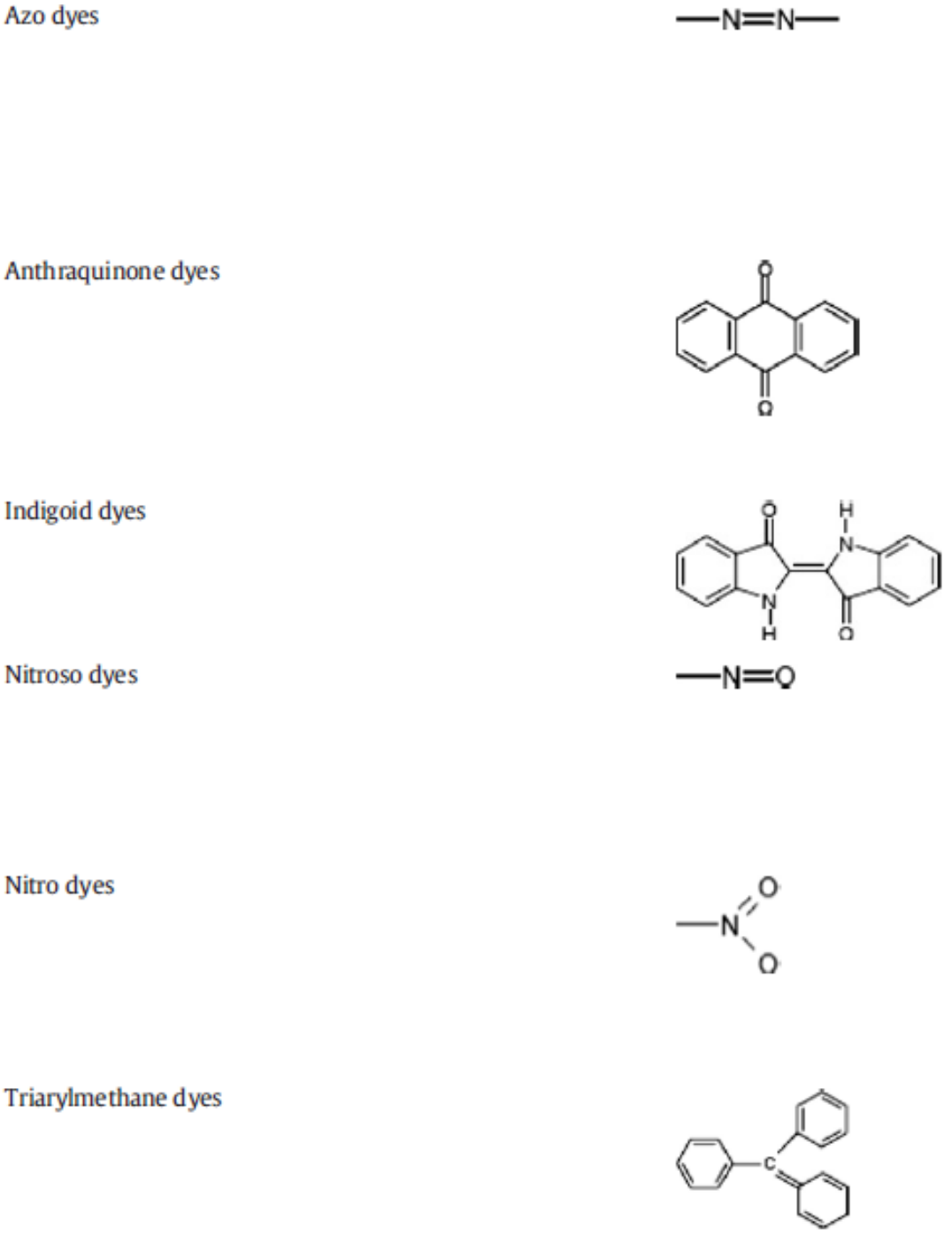

Figure 2.1. Chromophore of each type of dye according to their chemical structure (Yagub, Sen, Afroze, & Ang, 2014)

Regarding triarylmethane dyes, group in which brilliant green belongs to, they have three aryl groups (phenyls or heterocycles) bonded to a central carbon atom. This group have many applications, being mainly used for the dyeing of wool, silk, and cotton. In the medicine field, food and textile industries triarylmethane dyes are very used, as well as in the cosmetic and pharmaceutical industries. (Elvers, Hawkins, & Schulz, 2002), (Ricco, et al., 2020).

One of the dyes that is being studied in this Master Thesis is Orange II, a dye that belongs to azo dyes. Azo dyes have applications in industries like food, pharmaceutical or textile, being the most used group of dyes, with a quota of 60-70% of all the dyes produced in the world. One or more azo group (R_1−N=N−R_2) shape azo dyes and they have aromatic rings replaced mainly by sulfonate groups. (Wang, et al., 2021), (Swain, et al., 2021), (Balapure, Bhatt, & Madamwar, 2015).

Nevertheless, the chemical structure system has some complexities, so the system based on the applications is also widely used, being the one that the Colour Index applies principally.

- Acid
- Basic
- Direct
- Disperse
- Reactive
- Solvent
- Sulphur
- Vat

In the basic (cationic) dyes, it can be founded the methylene blue, one of the dyes that is going to be studied in this project. As they produced coloured cations in solution, they were given this name. Originally, this group was used for dyeing silk, wool and cotton but today they are usually bonded with substrates like paper, polyester, nylon, and inks. Aside from textile industry, is also used in the medicine field. (Elvers, Hawkins, & Schulz, 2002), (Yagub, Sen, Afroze, & Ang, 2014), (Gupta V. K., 2009).

2.2.3. Methylene Blue

Methylene Blue (CI Basic Blue 9, 52015), also known as methythioninium chloride or Swiss Blue, is a heterocyclic aromatic chemical compound which molecular formula is $C_{16}H_{18}ClN_3S$ and its molar mass is 319,85 g/mol. Belongs to the family of the basic (cationic) dyes. In its solid state, is a dark green crystalline powder. It is very soluble in water and its solution has a strong dark colour. Its chemical structure can be seen in the *Figure 2.2.* (PubChem, Methylene Blue Compound Summary, 2021)

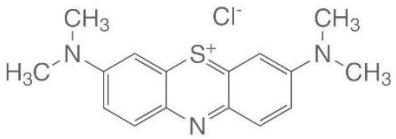

Figure 2.2. Methylene Blue structure (Thesnaar, Bezuidenhout, Petzer, Petzer, & Cloete, 2021)

Physicochemical properties of methylene blue are collected in the following table (PubChem, Methylene Blue Compound Summary, 2021):

Table 2.1. Physicochemical properties of Methylene Blue.

IUPAC name	[7-(dimethylamino)phenothiazin-3-ylidene]-dimethylazanium chloride
Other names	Basic Blue 9, Swiss Blue, Methylthionine Chloride, Urolene Blue
Appereance	Green powder in solid state
Molecular formula	$C_{16}H_{18}ClN_3S$
Molecular weight	319.85 g/mol
Colour Index	52015
Maximum absorption	665 nm
Solubility at 20ºC	40 g/L in water
Density	1 g/cm^3
Melting point	100 to 110 ºC
Toxic fumes	Nitrogen oxides, sulfur oxides and chloride (when heated to decomposition)
Chemical safety	Corrosive and irritant

Methylene blue was originally discovered by Heinrich Caro in 1876, who extracted methylene blue from aniline. It has a variety of applications in different fields.

Since its discovery was used in the textile industry, mainly employed for colouring silk, wool and cotton. Its high solubility and resistance characteristics justify its importance in this industry.

In this 19th century its antimicrobial properties were unveiled, becoming one of the mains antimalarial drugs and beginning to be used in the medicine field. In this area, has been widely used for the treatment of methemoglobinemia, cyanide poisoning, ifosfamide-induced encephalopathy, vasoplegia accompanied septic shock and urinary infection, though this last use is not recommended anymore. It is also applied during surgeries to colour body tissues in order to have a better visualization of them. Furthermore, methylene blue has antibacterial activity, being combined with other compounds or on its own. (Thesnaar, Bezuidenhout, Petzer, Petzer, & Cloete, 2021), (Ahmad & Aqil, 2008), (Hadi, Taheri, Amin, Fatehizadeh, & Gardas, 2021), (Geed, Samal, & Tagade, 2019).

Regarding its adverse effects, although it is not considered as a highly toxic chemical, methylene blue can cause anaemia, hypertension, nausea, abdominal and chest pain, methemoglobinemia, headache, eye burns or skin irritation. (Thesnaar, Bezuidenhout, Petzer, Petzer, & Cloete, 2021), (Hadi, Taheri, Amin, Fatehizadeh, & Gardas, 2021), (Geed, Samal, & Tagade, 2019).

2.2.4. Brilliant Green

Brilliant Green (CI 42040), also known as Basic Green 1, is a cationic dye, which in its solid form is a green crystalline powder. Regarding its molecular weight, is heavier than the methylene blue, weighting 482,63 g/mol. (PubChem, Brilliant Green Compound Summary, 2021). It is soluble in alcohol and water and it is mainly used in the leather, textile, biological, rubber and plastic industries. Its toxicity and carcinogenicity are the main concerns with this dye being present in wastewater. (Bhattacharya, et al., 2019), (Khan, et al., 2020), (Rehman, et al., 2018).

This dye is included in the triarylmethane group, since the triphenylmethane group is the chromophore (see *Figure 2.3)*

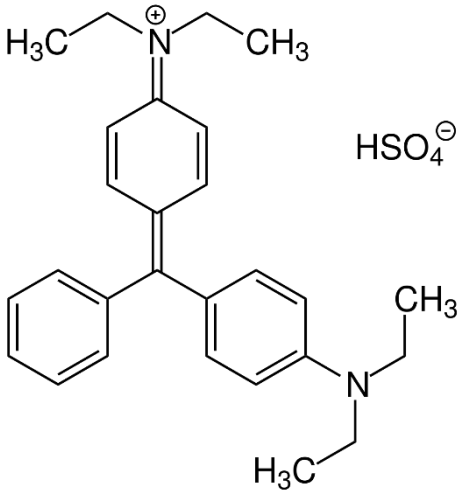

Figure 2.3. Brilliant Green structure (Bhattacharyya & Sarma, 2003)

Physicochemical properties of BG are collected in the following table (*Table 2.2*) (Elvers, Hawkins, & Schulz, 2002), (PubChem, Brilliant Green Compound Summary, 2021), (Brilliantgrün stoffdaten, 2021), (Bhattacharyya & Sarma, 2003):

Table 2.2. Physicochemical properties of Brilliant Green

IUPAC name	4-{[4-(Diethylamino)phenyl](phenyl)methylene}-N,N-diethyl-2,5-cyclohexadien-1-iminium hydrogen sulfate
Other names	Basic Green 1, Malachite Green G, Emerald Green, Zelyonka
Appereance	Green crystalline powder in solid state

Molecular formula	$C_{27}H_{34}N_2O_4S$
Molecular weight	482.63 g/mol
Colour Index	42040
Maximum absorption	624 nm
Solubility at 20ºC	100 g/L in water
Density	1.126 g/cm^3
Melting point	210 ºC
Toxic fumes	Nitrogen oxides, ammonia and sulfur oxides (when heated to decomposition)
Chemical safety	Corrosive, Acute Toxic, Irritant and Environmental Hazard

Brilliant Green was first discovered in Germany in 1979 and is synthesized from benzaldehyde and diethylaniline (Elvers, Hawkins, & Schulz, 2002)

Aside from being used in the textile, rubber, and plastic industries, among others, is also used in the fish farming industry, since its anti-microbial, anti-parasitic and anti-fungal properties, is useful for treating certain fish illness, being also economical. (Damirchi, Maliheh, Heidari, Es' haghi, & Chamsaz, 2019)**.**

With regard to its adverse effects, it can be carcinogenic and mutagenic in humans, as well as in animals. Therefore, is not authorized as a valid medication in the European Union and in the United States. In addition, Brilliant Green can cause eye burns, gastrointestinal issues if swallowed (nausea, vomiting and diarrea), lungs, kidney and heart problems and can be also responsible of harming the respiratory tract when inhaled. For all these reasons, it is mandatory to remove this compound from the wastewater. (Bhattacharya, et al., 2019), (Khan, et al., 2020), (Rehman, et al., 2018), (Bhattacharyya & Sarma, 2003)**.**

2.2.5. Acid Orange 7

Also known as Orange II or C.I. 15110, is an azo dye which is mainly used in the cosmetic, nylon, detergent, wool, and paper printing industries. In its solid state is an orange powder and is a dye that shows a high stability with the light and temperature. (Luo, Yartym, & Hepel, 2002)**.**

Due to its complex structure (see *Figure 2.4*) and its stable properties is a pollutant that presents many difficulties to remove it from the wastewater (Wang, et al., 2021).

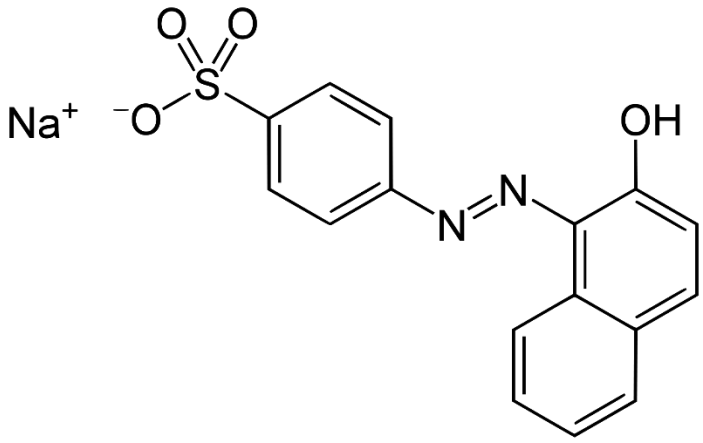

Figure 2.4. Acid Orange 7 structure. (Heibati, et al., 2015)

In the following table, physicochemical properties of Orange II are shown (*Table 2.3*). (Wang, et al., 2021), (Swain, et al., 2021), (PubChem, Acid Orange 7 Compound Summary, 2021), (Orange II stoffdaten, 2021), (Heibati, et al., 2015).

Table 2.3. Physicochemical properties of Orange II

IUPAC name	4-(2-hydroxy-1-naphthylazo) benzenesulfonic acid sodium salt
Other names	Acid Orange 7, β-naphtol Orange, Acid Orange A
Appereance	Orange powder
Molecular formula	$C_{16}H_{11}N_2NaO_4S$
Molecular weight	350.83 g/mol
Colour Index	15110
Maximum absorption	484 nm
Solubility at 30ºC	116 g/L in water
Density	1,6 g/cm^3
Melting point	164 ºC
Toxic fumes	Carbon monoxide, carbon dioxide, nitrogen oxides, sulfur oxides
Chemical safety	Toxic

Its carcinogenicity and toxicity have been proved, so its removal from wastewater is a priority. Aside from being harmful for humans, whom it may cause anemia, respiratory infection, skin disease, or another health issues, it can also be dangerous for the aquatic species (Swain, et al., 2021).

Inside azo dyes, Orange II belongs to monoazo dyes, which are used for dying wool, paper, food, soaps, and cosmetics, as mentioned before. Besides being used in these areas, and because of its low cost, it is also used for colouring leather and for manufacturing colour lakes (Elvers, Hawkins, & Schulz, 2002).

2.2.6. Effects on the environment and health caused by the dye spill on wastewater

As it has been shown in the previous sections, dyes can have a negative effect on our health as well as in the environment. As years go by, more and more dyes are being produced over the world in industries such as pulp mills, dyestuff, distilleries, tanneries, and textile. (Pavithra & Jaikumar, 2019). Annually, it is estimated that the production of dyes is more than 7 x 10^5 tones. (Chanikya, Nidheesh, Babu, Gopinath, & Kumar, 2021).

Specifically, the textile sector, which mainly uses dyes, is one of the most pollutants among the industries, as it is a sector which uses huge amounts of water (200-400 L per kg of fabric) (Yukseler, et al., 2017), and about 10-15 % of the dyes used in these industries are poured into the wastewater (Selvakumar, Manivasagan, & Chinnappan, 2013). This sector is especially contaminating in developing countries like India. In this country, 50% of the dyestuff used in an average textile is emitted into the water effluent. (Xiao, Liu, & Ge, 2021). This dye contamination can cause severe issues in human health, as well as in other living beings health, like aquatic organisms.

As written in the previous paragraphs, several kinds of dyes have carcinogenic, mutagenic, and allergic effects on human beings, due to their toxic nature (Gupta, Pathania, Kothiyal, & Sharma, 2014).

Regarding aquatic organisms, dyes in water systems (even at very low concentrations) gives colour to these systems, which leads to an increased chemical oxygen demand, suspended solids and, as dyes can absorb visible light on a large scale, blocks the penetration of light into water. This means it would be more complicated to aquatic plants to do the photosynthesis. In conclusion, this type of pollutants causes an ecological imbalance in aquatic ecosystems. (Chanikya, Nidheesh, Babu, Gopinath, & Kumar, 2021), (Gupta, Pathania, Kothiyal, & Sharma, 2014).

As for basic, cationic and azo dyes, its discharge into the wastewater is one of the main ecological problems. It is estimated that around 70% of all the dyes used commercially are azo dyes, and more than 10% of approximately 1 million tons of azo dyes that are produced worldwide in industries such as textile, pharmaceutical or food industries is released into the water. (Wang, et al., 2021), (Swain, et al., 2021), (Heibati, et al., 2015). The harmful effects of these three kinds of dyes goes from causing skin diseases, anaemia, diarrhoea, hypertension and several more illnesses, as it was mentioned in the previous sections.

2.3. Dyes removal methods

Nowadays, recovering and reusing wastewater is one of the most urgent problems in our society. As clean water sources are being quickly drained, and dyes have several side effects due to its noxiousness, it is needed that these synthetic dyes do not blend with water sources.

Not only these dyes can cause diseases such as cancer, respiratory infections, diarrhoea and others, but these dye effluents are filled with other hazardous chemicals like sulphuric acid, acetic acid, hydrogen peroxide, hydrochloric acid, etc. Consequently, the development of removal methods which can erase efficiently these dyes without producing more secondary pollution is compulsory. This efficiency is of utter importance, as with very low concentrations (around 1 mg/L) these dyes are noticeable in the wastewater. (Heibati, et al., 2015), (Katheresan, Kansedo, & Lau, 2018).

Researchers have found several removal methods, but there is no ideal method for the time being, as this issue have been investigated for the last 30 years only. Besides, removing dyes from wastewater is complex, as synthetic dyes are made to be very stable structures (due to the presence of auxochromes, which makes them soluble in water, and chromophores, colour giving compound), in order to fix them better to the textile materials. But as it can be seen, this attachment is not completely achieved: around 20% of dye and chemical molecules used in the textile industry are not able to be absorbed by the textile materials, being this number 75% in the case of fabrics (Pavithra & Jaikumar, 2019), (Katheresan, Kansedo, & Lau, 2018).

In the table below (*Table 2.4*), a short summary of the main removal methods will be explained, describing them along with their advantages and disadvantages based on various parameters such as the cost, the energy consumption, the wastes produced or their efficiency when removing these dyes.

Table 2.4. Removal methods for dyes in wastewater (Pavithra & Jaikumar, 2019), (Katheresan, Kansedo, & Lau, 2018).

Method	Description	Advantages	Disadvantages
Biological treatments	Removal of dyes with microorganisms with the ability to degrade these substances	Inexpensive Eco-friendly High efficiency	System instability Does not completely eliminate all hazardous particles
Adsorption	Transference of dyes from wastewater to the surface of a highly porous solid material	Simplicity Low cost Wide range of dyes	Adsorbents can be expensive
Coagulation and flocculation	Clumping of dyes produced by coagulation agents. Clumps are eliminated using filtration.	Simple to operate Effective against a wide range of dyes	Can be expensive High production of sludge
Ion exchange	Interchange of ions between the dye wastewater and the surface of an insoluble solid material	Solid can be regenerated and reused Able to remove soluble dyes	Not efficient for every dye Expensive
Electrocoagulation	Agglomeration of pollutants produced by the ions released by iron or aluminium anodes	Low cost Low production of sludge	Not effective with every dye
Photocatalytic process	Degradation of dyes by using UV light	No sludge production Highly effective	Production of aromatic amines
Advanced oxidation process	Removal of dyes through the generation of oxidants and hydroxyl radicals	Able to remove toxic materials and dyes in unusual conditions	Expensive
Ozonation	Degradation of dyes through ozone	High effective No sludge production	Expensive Toxic by-products High energy required

Finally, as it is the method used in this work, nanofiltration will be further explained in the following section.

2.3.1. Nanofiltration (NF)

Nanofiltration is the membrane process where particles from 1 to 10 nanometres size are separated from the effluent when it is passed through a thin-pored membrane. These membranes are thin-film composite, and its mechanism is based in electrostatic repulsion, being able to remove almost 98% of dyes in wastewater. (Katheresan, Kansedo, & Lau, 2018), (Technical Manual: FILMTEC Reverse Osmosis Membranes, 2016), (Buscio, et al., 2016).

In the nanofiltration process, the stream which has been purified from the feed water is called permeate, and the concentrated stream is known as the retentate. (Technical Manual: FILMTEC Reverse Osmosis Membranes, 2016)

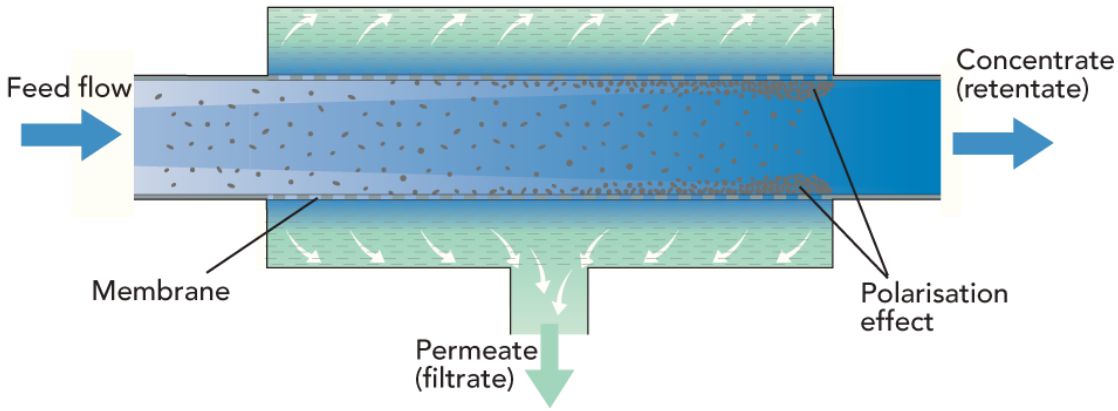

Figure 2.5. Nanofiltration membrane mechanism. Modified from (Pavithra & Jaikumar, 2019)

The main advantages of nanofiltration are its high efficiency, the ability to remove any type of dye and, despite having an initial high cost, its overall price is not so expensive, as the permeate can be reuse in the process, as well as some concentrate dyes (Pavithra & Jaikumar, 2019), (Katheresan, Kansedo, & Lau, 2018), (Buscio, et al., 2016), (Hassani, et al., 2008).

It is known that permeate flux (rate of permeate transported per unit of membrane area in L/m^2h) and salt rejection (percentage of solute concentration removed from the feed by the membrane) are the parameters which influence the most the nanofiltration performance, and these parameters are mainly affected by some factors (Katheresan, Kansedo, & Lau, 2018), (Technical Manual: FILMTEC Reverse Osmosis Membranes, 2016):

- Pressure

- Temperature
- Recovery
- Feed water salt concentration

Finally, there are other types of membrane treatments such as reverse osmosis (RO) or ultrafiltration (UF), being the nanofiltration between these two methods in terms of particles separation size. Nanofiltration proves to be better method that these other two because it presents less fouling (defined as "the accumulation of foulants on the or into the membranes and which degrades the selectivity as well as the permeability of the polymeric membranes"), it is capable of removing a higher percentage of dyes and having fewer limitations when it comes to the operating pressure. (Pavithra & Jaikumar, 2019), (Buscio, et al., 2016).

2.3.1.1. Nanofiltration working principle

As nanofiltration membranes are needed to be avoided from having particles accumulated on their surface, the operation mode for this kind of membranes is called cross-flow. The feed stream flows in parallel with the membrane layer, preventing the cake layer (the layer which is formed with the precipitation of the solutes) to increase more quickly, prolonging the operational time of the membrane (Gholami, Nasseri, Alizadehfard, & Mesdaghinia, 2003), (Mendez, 2019).

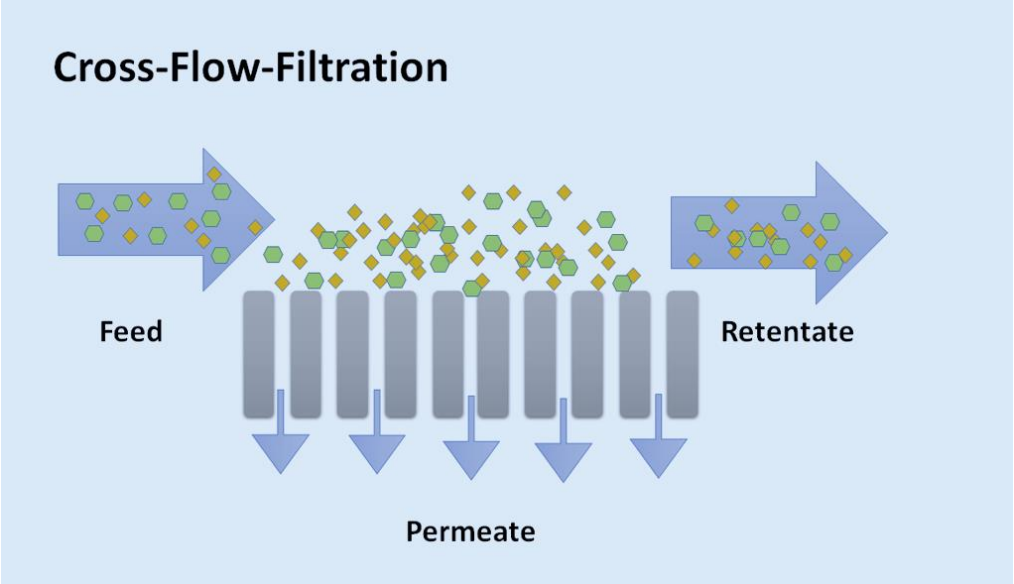

Figure 2.6. Ilustration of how cross-flow filtration mode works. Modified from (Technical Manual: FILMTEC Reverse Osmosis Membranes, 2016)

Another advantage of this kind of operation mode, is that the solutes precipitated in the membrane surface are partially rinsed because of the high shearing forces of this flow. (Hohm, 2019).

2.3.1.2. Concentration polarization

As the nanofiltration process is taking place throughout the time, some solutes are not transported to the permeate stream, staying on the membrane surface. These solutes are supposed to be rinsed by the retentate stream, but as the velocity on the membrane surface is almost non-existent, they can only go to the retentate stream through diffusion. This diffusion takes place in the opposite way of the feed stream, resulting in the formation of an area where the solute concentration is higher than in the rest of the solution. This area, with a concentration gradient, is known as the boundary layer. (Legaz, 2016).

This situation is called membrane polarization, and the raise of concentration that occurs in the solution in contact with the membrane surface is called concentration polarization. (Legaz, 2016), (Banerjee & De, 2010).

Concentration polarization is one of the main problems that appears when working with nanofiltration membranes, which are activated through pressure, since it increases the resistance to transport the solutes from the feed stream. In *Figure 2.7* it can be observed the formation of these layers which could affect the correct operation of the nanofiltration membrane. (Banerjee & De, 2010).

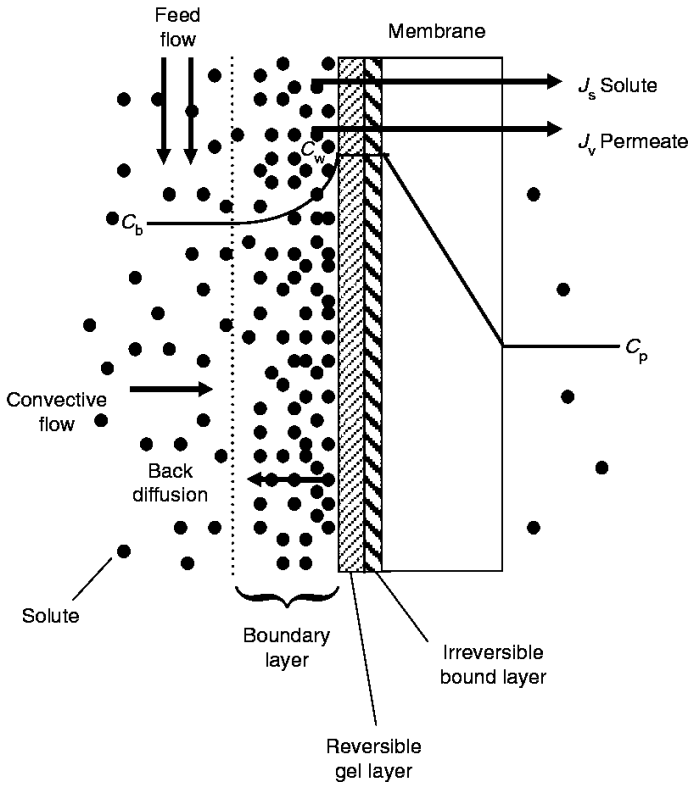

Figure 2.7. Formation of concentration layers. Modified from (Technical Manual: FILMTEC Reverse Osmosis Membranes, 2016)

Cross-flow velocity, feed water composition or permeate flux are some factor which could affect the concentration gradient in the boundary layer. (Mendez, 2019).

3. Materials and methods

In this chapter a description of the different materials, equipment and analytic methods employed, will be explained.

3.1. Materials

As mentioned in the section 2.2, three dyes, which has been mixed with distilled water, have been studied:

- Methylene Blue (supplied by Merck KGaA)
- Brilliant Green (supplied by Sigma-Aldrich)
- Acid Orange 7 (supplied by Carl Roth GmbH)

3.2. Equipment

3.2.1. Nanofiltration pilot plant (NFPP)

To proceed with this investigation, a nanofiltration pilot plant located in the Institute of Wastewater Management and Water Protection (AWW) at TUHH was used.

This pilot plant drives, with the help of a feed pump, a feed solution through a semipermeable membrane. Firstly, this feed is transferred to a heat exchanger and then it is moved through the pipes to the nanofiltration module. In this investigation, the pre-filters and the NF module were not used. The parts of the NFPP that were used can be seen in the *Figure 3.1.*

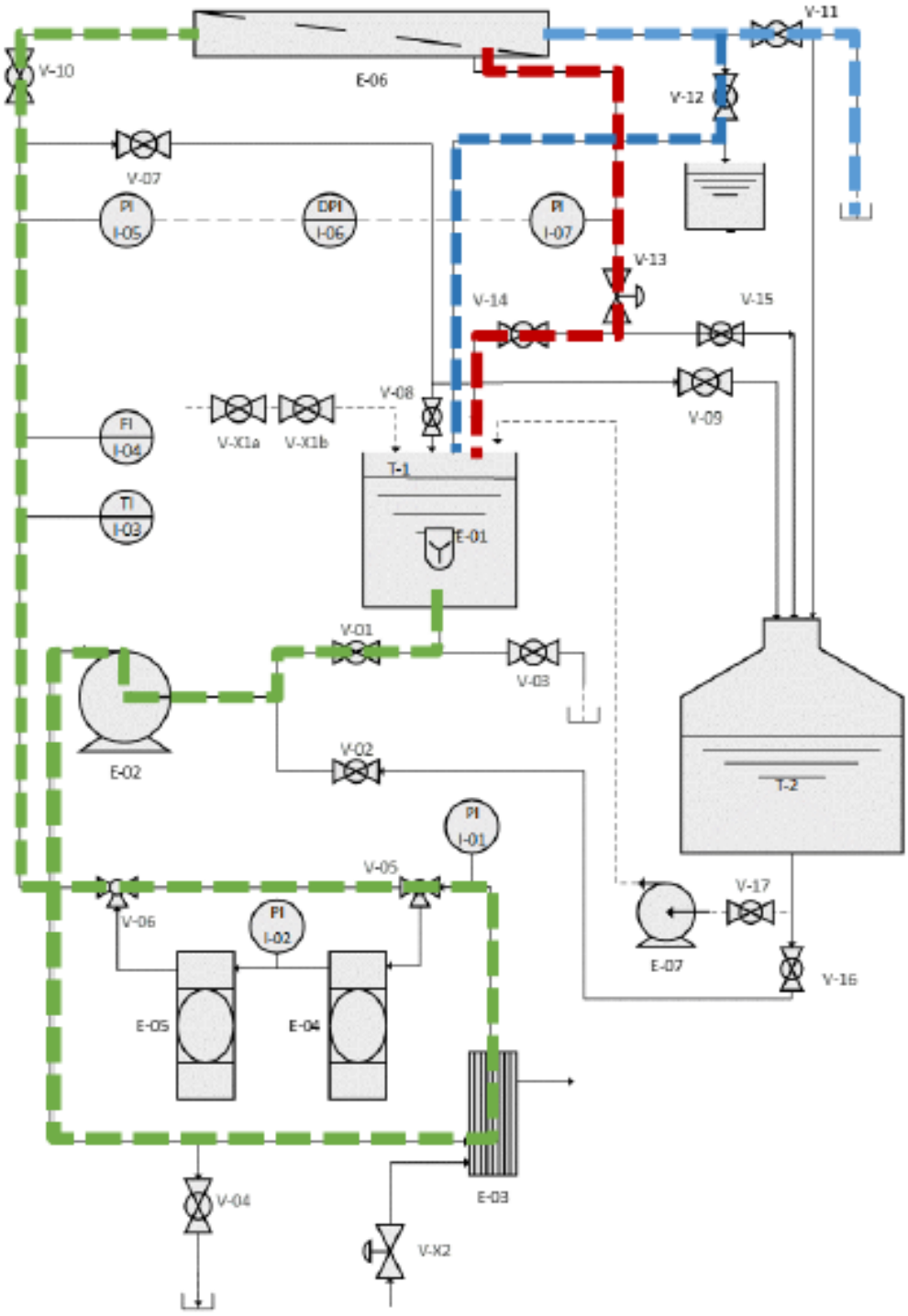

Figure 3.1. Direct nanofiltration without prefiltration with feed vessel (T-1). (Hohm, 2019)

In this pilot plant two modes can be used: batch mode or continuous operation mode (full recycling) which is the one that it was used in this investigation. In full recycling mode, the streams that comes out of the permeate and the retentate are recirculated back into the feed vessel, allowing to do long-term operations (as it happens in this investigation).

3.2.2. Membrane

The membrane used in the nanofiltration module is the model Filmtech™ NF270-2540 from DOW Chemical Company. This membrane is made of polyamide thin-film composite, which is divided into three layers: a polyester support web, a microporous polysulfone interlayer, and an ultra-thin polyamide barrier layer on the top surface. This polyamide layer curbs the hydrophobicity of the membrane, due to polyamide compounds have amide and carboxyl groups bound to the aromatic rings. (Hassani, et al., 2008)**.**

This membrane is built as a spiral-wound, which is inside a cylindrical pressure vessel *(see*.*Figure 3.2* and *Figure 3.3*). This vessel is able to work with a pressure up to 69 bar (1000 psi) and can hold a 2.5" element.

In *Table 3.1* the membrane specifications are summarised and in *Table 3.2.* its operating limites are defined.

Table 3.1. Summary of membrane specifications

Characteristics of membrane	**Description**
Active Area	2.6 m^2
Applied Pressure	4.8 bar
Permeate Flow Rate*	3.2 m^3/d
Typical Stabilized Salt Rejection*	< 97 %

*based on the following test conditions: 2000 ppm MgSO4, 25ºC and 15 % recovery at above specified pressure

Table 3.2. Operating limits of the membrane

Parameters	**Description**
Maximum Operating Temperature	45 ºC
Maximum Operating Pressure	41 bar
Maximum Feed Flow Rate	1,400 L/h
Maximum Pressure Drop	0.9 bar
pH Range, continuous Operation	2-11
pH Range, short-term Cleaning (·30min)	1-12

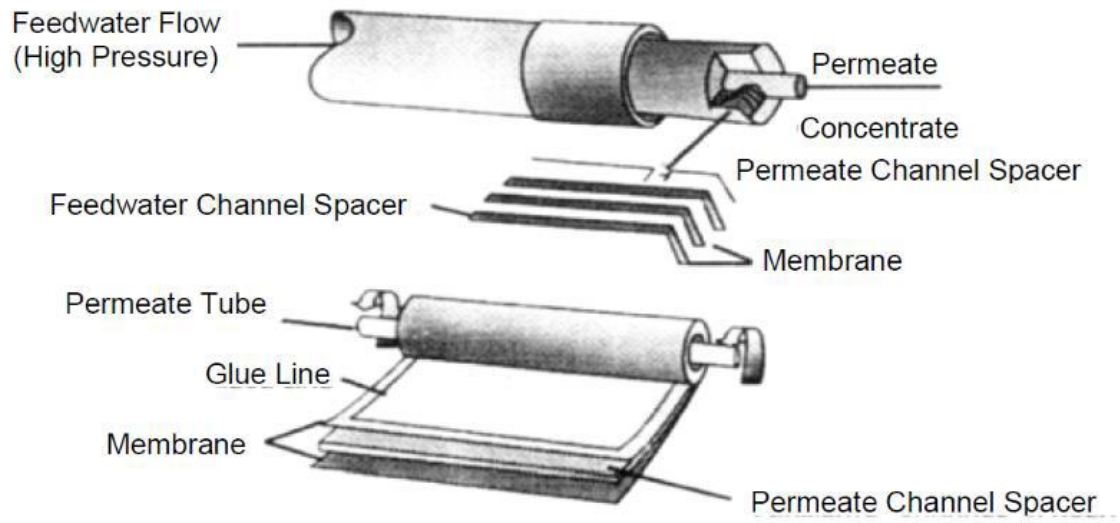

Figure 3.2. Spiral-wound membrane module (Technical Manual: FILMTEC Reverse Osmosis Membranes, 2016)

Figure 3.3. Close-up view to the cylindrical vessel which contains the membrane

3.3. Methods

To determine the concentration of each one of the three dyes studied, a UV-visible spectrophotometer supplied by JASCO GmbH was used. This spectrophotometer is located in the main lab of the Institute of Wastewater Management and Water Protection (AWW) at TUHH.

In this spectrophotometer it was measured the absorption of solutions with a known concentration of each dye in a range from 190 to 900 nm. A volume of around 3 mL of these solutions were introduced in a quartz cuvette provided by Carl Roth GmbH, being compared with the absorption of another cuvette filled with distilled water. Every solution was measured with two cycles.

As each dye has a different maximum absorbance value, it is necessary to present each one of them in three different sections.

3.3.1. Determination of Methylene Blue concentration

In the first place, as the maximum absorbance value detected in the spectrophotometer is 3, the 10 mg/L solution (the maximum concentration that it was prepared) was measured firstly to check that the absorbance was within the spectrophotometer limit. This value was 1.706, so it was not needed to dilute more the solution. (see *Figure 3.4*)

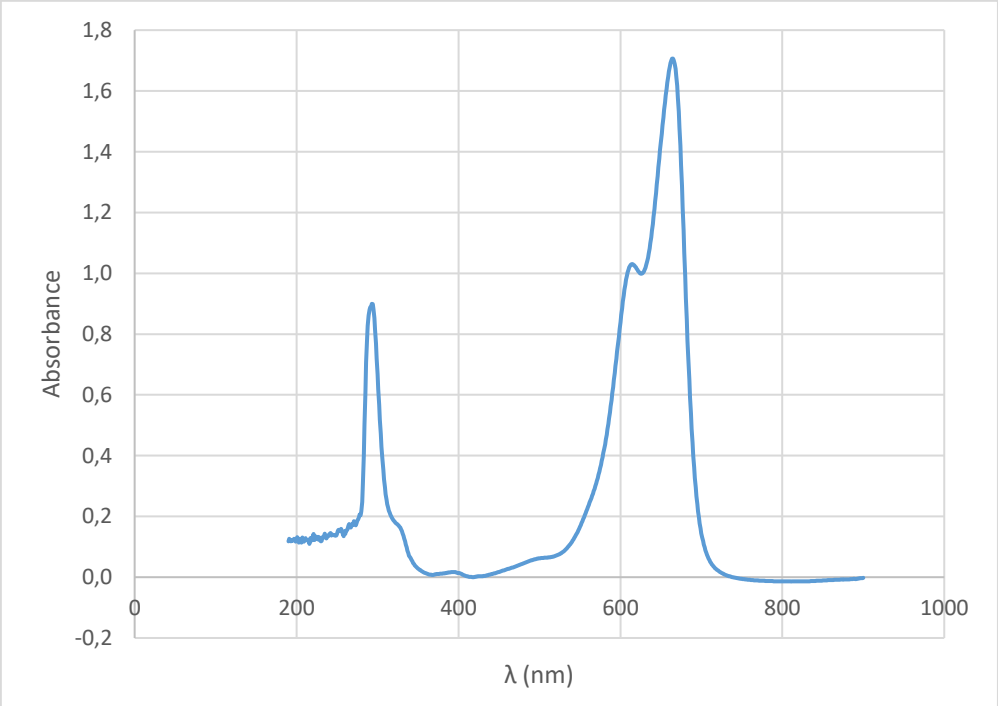

Figure 3.4. Absorbance vs wavelength (nm) for a 10 mg/L solution of Methylene Blue

As it can be seen in the figure, the wavelength of maximum absorbance was at 665 nm

In order to know the concentration of methylene blue in the water at pH around 7, the calibration curve had to be calculated.

The concentrations of Methlyene Blue in the prepared solutions were the following: 0.5, 0.6, 0.7, 0.75, 0.8, 0.9, 1, 2, 2.5, 3, 4 and 5 mg/L (the solution of 3 mg/L were discarded because the value of the absorbance was not linear with the rest of the solutions). These solutions were prepared from a solution of 10 mg/L, which was obtained dissolving 10 mg of solid Methylene Blue into a 1 L flask of distilled water. The absorbance and concentrations values used for the calibration curve are collected in the Appendix A, section 7.1.

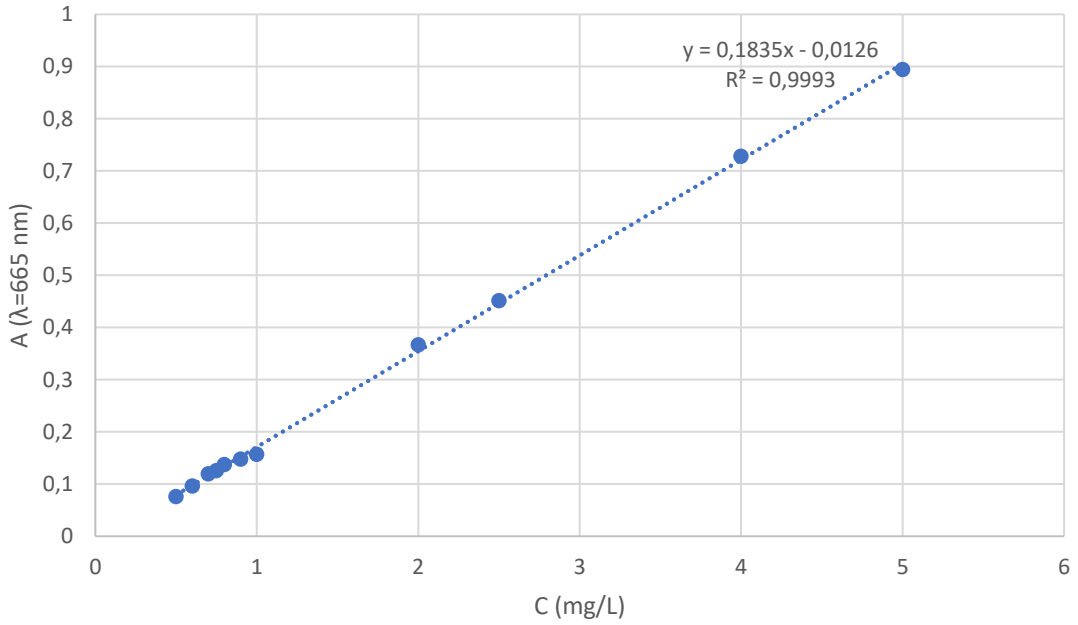

Figure 3.5. Calibration curve for Methylene Blue dissolved in distilled water

3.3.2. Determination of Brilliant Green concentration

First of all, it had to be check what was the wavelength of maximum absorbance and that the absorbance value at 10 mg/L (solution of higher concentration) was within the limits (absorbance of 3). As it can be seen in the *Figure 3.6.*, this value was 2.43171, with a wavelength of 624 nm.

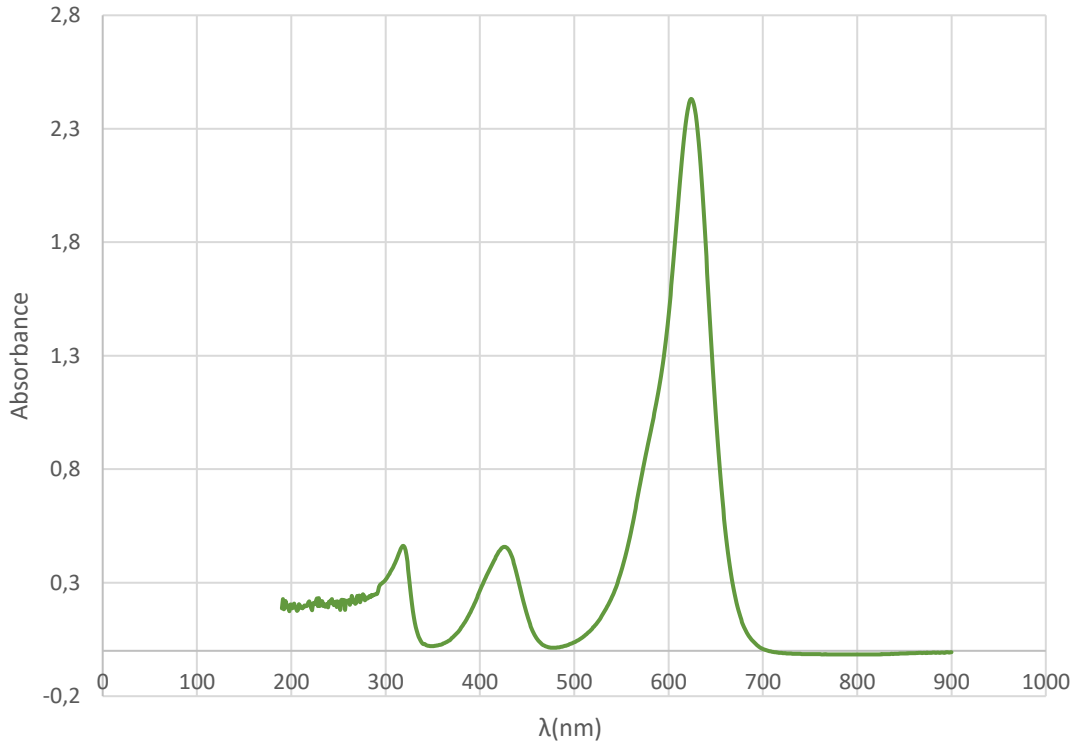

Figure 3.6. Absorbance vs wavelength (nm) for a 10 mg/L solution of Brilliant Green

To determine the concentration of Brilliant Green, two calibration curves had to be drawn, one for the lower concentrations, and one for the higher concentrations, both at pH around 7.

The concentrations of the solutions used for the lower concentration calibration curve were: 0.05, 0.25, 0.5, 1, 2 and 3 mg/L. They were prepared from a solution of 1 L flask with distilled water in which it was dissolved 10 mg of Brilliant Green. The absorbance and concentration values can be seen below in the calibration curve.

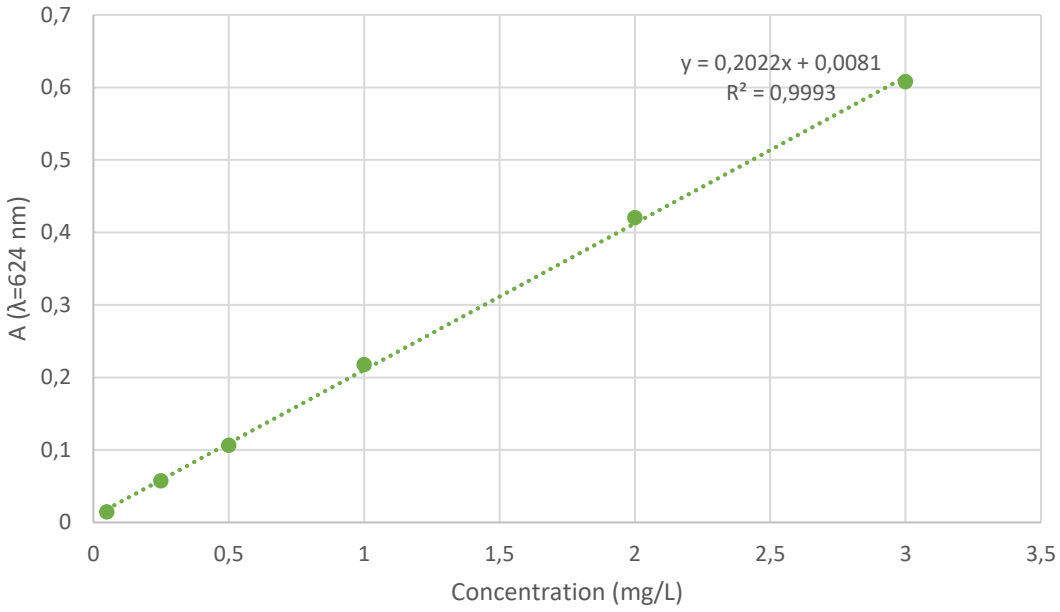

Figure 3.7. Calibration curve for Brilliant Green dissolved in low concentrations in distilled water

With respect to the higher concentration calibration curve, the following solutions were prepared: 0.25, 0.4, 0.5, 0.6, 0.8, 1, 2, 3, 4 and 5 mg/L. As well as in the lower concentration calibration curve, these solutions were prepared from a solution of 1 L flask with distilled water in which it was dissolved 10 mg of Brilliant Green. Below are shown the absorbance and concentration values measured for this curve.

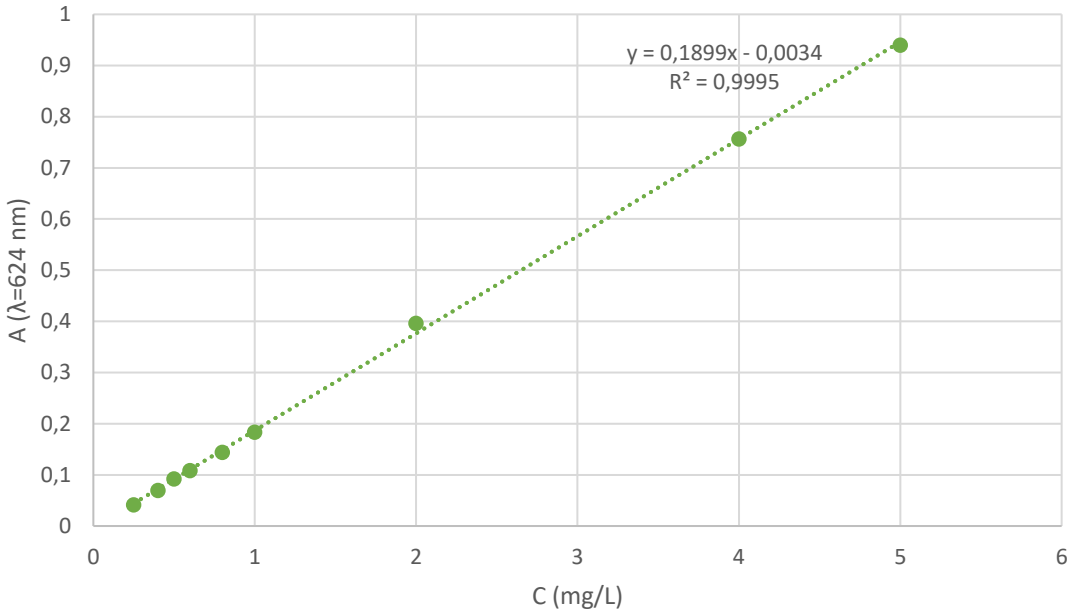

Figure 3.8. Calibration curve for Brilliant Green dissolved in high concentrations in distilled water

3.3.3. Determination of Acid Orange 7 concentration

Firstly, as it was conducted in the previous sections, the absorbance of Orange II in the solution with the highest concentration had to be checked. This time, the concentration of this solution was 20 mg/L instead of 10 mg/L because at 10 mg/L the absorbance was too low. Once measured and checked that the absorbance of the 20 mg/L solution was within the limits (A = 1,06039, λ = 484 nm) the calibration curve could be determined.

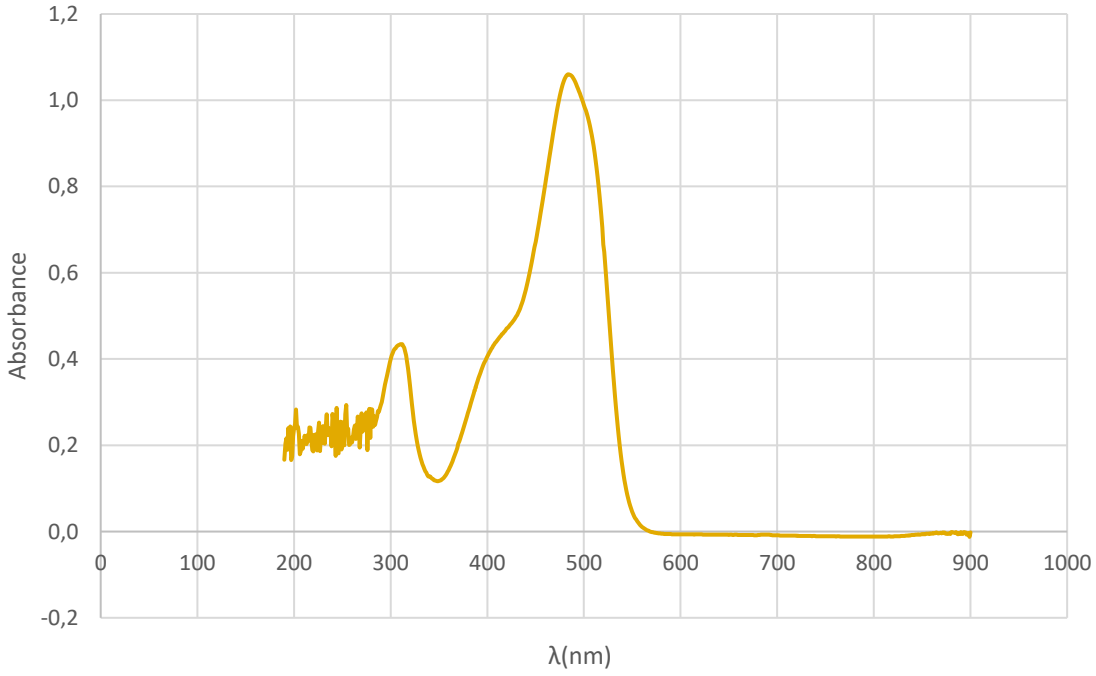

Figure 3.9. . Absorbance vs wavelength (nm) for a 20 mg/L solution of Acid Orange 7

Measured at pH around 7, the concentrations of the solutions used for this calibration curve were:0.25, 0.5, 0.75, 1, 2, 3, 4, 5, 6, 7, 8, 9, 10, 12, 14, 16, 18, 20. As it was made in the other dyes, they were prepared from a solution of 1 L flask with distilled water in which it was dissolved 20 mg of Brilliant Green. The absorbance and concentration values can be seen below in the calibration curve.

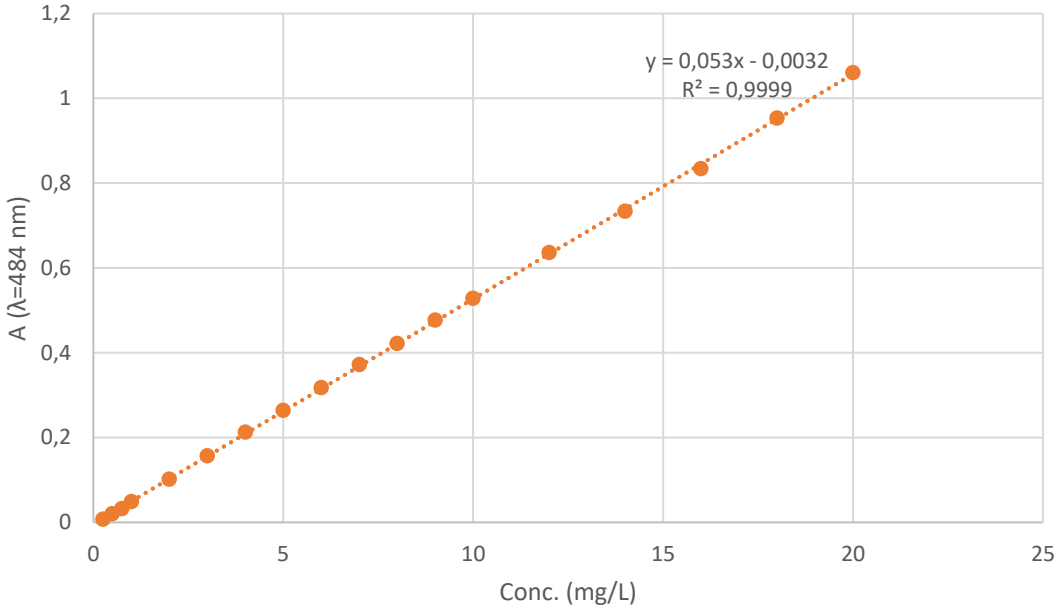

Figure 3.10. Calibration curve for Acid Orange 7 dissolved in distilled water

3.3.4. Experimental procedure and sampling

When starting the experiment, the feed tank was filled with a 80 L solution of distilled water with the corresponding dye. In every case, the initial concentration of the feed tank was 50 mg/L,the pH was around 7 and the temperature was oscillating around 20 ºC. The distilled water was use instead of tap water because when Brilliant Green dye was mixed with tap water, around 24 hours later, the colour of the solution changed to an unusual blue colour.

Each one of the experiments had a duration of 4 hours and a half, changing the pressure or the feed flow values every 30 minutes. A sample of each one of the streams (permeate, retentate and feed) was taken in a 15 minute interval. In these samples it would be measured the absorbance, as well as the pH. Furthermore, every 30 minutes it would be timed in how much time were filled the container in where the sample were taken, being weighed after that.

3.3.5. Chemical cleaning

Between the conduction of each experiment, the membrane had to be chemically cleaned in order to remove the colour from its layers. After doing the first experiment with methylene blue, it was observed that the permeate and retentate streams had still

some blue colour in it, even after flushing the system with distilled water for a whole day.

Therefore, after emptying the feed tank and flushing the system with distilled water for several hours, the membrane was cleaned chemically in two steps:

- First of all, a NaOH solution with a concentration of 0.01 wt% was prepared. In the pilot plant manual it is recommended to clean the membrane with a 0.1 wt% NaOH solution, but in this case the pH was beyond 12 (around 13, more specifically), what is a high pH which could damage the membrane in long-term flushings. The solution with this lower concentration, 0.01 wt%, it was able to maintain a constant pH of 11.5, which was a better option for the membrane. After preparing it and checking the pH was not dangerous for the membrane, it was introduced around 80 L of this solution into the feed tank. Then, a short flushing of two minutes was done, letting the solution soaking the nanofiltration module afterwards for an hour. Finally, a recirculation of the cleaning solution was performed for around 30 minutes, disposing it after this last step was completed.
- After the NaOH solution, a HCl solution with a concentration of 0.02 wt% was prepared. As it happens with the NaOH solution, the nanofiltration pilot plant manual recommended a higher concentration (0.2%), but in this case the pH was below 2, which also could be harmful for the membrane. With the 0.02 wt% the pH was constant and was oscillating around 2.3. After elaborating it and checking the pH was beyond 2, around 80 L of this solution was introduced into the feed tank. Then, as it was done with the NaOH solution, a two-minutes flushing was performed, allowing the solution to soak the membrane for an hour after this short flushing. Eventually, and during 30 minutes, a recirculation of the cleaning solution was done, disposing it after this last step was completed.

In the case of Orange II, the first step had to be repeated because after these two steps, it could be observed that the water coming out of the system was still a little bit orange.

Other cleaning solutions were prepared to check what was the best procedure to clean the membrane. For instance, a H_2O_2 solution of 0.2 wt% or solutions with NaOH or HCl with higher concentrations, but the solutions used were proven to be the best removing the colour and the least harmful for the membrane.

3.3.6. Study of nanofiltration

In order to analyse how was the performance of the nanofiltration membrane, a series of experiments were performed, varying some parameters which could have an influence in this performance. The results of these experiments could be seen in the *Appendix A*

3.3.6.1. Study of feed pressure influence

To establish the influence of feed pressure in the nanofiltration of dyes in distilled water, this pressure was modified from 2 to 4 bars, checking that the other parameters, such as the feed flow (L/h), the temperature or the pH were constant during all the experiment.

Every experiment was run with an initial concentration of 50 mg/L of the dye, a temperature around 20 ºC, a pH over 7 and a duration of 4 hours and a half.

In order to run the experiments, 4 mg of solid dye was introduced in the feed tank and 80 L of distilled water were mix with this dye. This solution was mingled with a stirrer at a medium speed for around 30 minutes.

During the experiment, every 15 minutes a sample was taken from the feed tank, and from the retentate and permeate streams. For this purpose, it was used 20 mL vials, which were weighed afterwards to check the volume collected. Finally, the absorbance of these solutions were measured in order to calculate the dye concentrations in them.

3.3.6.2. Study of feed flow influence

With the aim to establish the influence of feed flow influence in the nanofiltration of dyes in distilled water, this parameter was modified from 100 to 200 L/h, checking that the other parameters, such as the feed pressure (bar), the temperature or the pH were constant during all the experiment.

Every experiment was run introducing 4 mg of solid dye into the feed tank, where 80 L of distilled water were mix with this dye with the help of a stirrer for over half an hour.

Every experiment was run with an initial concentration of 50 mg/L of the dye, a temperature around 20 ºC, a pH over 7 and a duration of 4 hours and a half.

As stated in the previous section, these experiments were performed with an initial concentration of 50 mg/L of the dye, a temperature around 20 ºC, a pH over 7 and a duration of 4 hours and a half.

As long as these experiments were running, a sample every 15 minutes was taken from the feed tank, and from the retentate and permeate streams as well. To achieve it, 20 mL vials were used, which were weighed afterwards to check the volume collected. At last, the absorbance of these solutions were measured in order to calculate the dye concentrations in them.

3.3.7. Treatment of experimental data

3.3.7.1. Volumetric measurement

Retentate flow Q_R as well as permeate flow Q_P are measured by filling a little jar, which had been weighed before running the experiment, and using a chronometer to know in

how much time this jar was filled. After filling it, the jar would be weighed again in order to calculate the weight of the permeate and the retentate.

It has been assumed that the density *ρ* of both retentate and permeate was the same as distilled water (*ρ≈1 kg/L at 20ºC)*, as they were low concentrated.

Equation (1) was used to calculate the flows of both streams (Legaz, 2016), (Abid, Zablouk, & Abid-Alameer, 2012), (Hohm, 2019)**.**

$$Q\left(\frac{L}{h}\right) = \frac{V(L)}{t(h)} = \frac{m(kg)}{\rho\left(\frac{kg}{L}\right) * t(h)} \approx \frac{m(kg)}{t(h)} \quad (1)$$

Where:

m: weight of the jar with the permeate or the retentate inside (kg)

t: time lapse until the jar was filled with the permeate or the retentate (h)

3.3.7.2. Rejection factor R

This parameter relates the solute concentration in the permeate stream (mg/L) with the solute concentration in the feed stream (mg/L).

This parameter defines the membrane ability to remove the solute and the quality of permeate.

Equation (2) was used to calculate the rejection factor (Legaz, 2016), (Abid, Zablouk, & Abid-Alameer, 2012), (Hohm, 2019)**.**

$$R = \left(1 - \frac{C_P}{C_F}\right) * 100 \quad (2)$$

Where:

R: rejection factor (%)

C_P: the solute concentration in the permeate stream (mg/L)

C_F: the solute concentration in the feed (mg/L)

3.3.7.3. Permeate flux J_W

It is a parameter that describes the liquid flow through the membrane. It is defined by the flow, the solution salinity and the membrane's pore size.

Permeate flux is the volumen of solution that goes through the membrane per unit of time and the specific area of the nanofiltration membrane.

Equation (3) was used to determine the permeate flux (Legaz, 2016), (Abid, Zablouk, & Abid-Alameer, 2012), (Hohm, 2019)**.**

$$J_W = \frac{Q_P}{A} \tag{3}$$

Where:

J_W: permeate flux (L/(m^2·h))

Q_P: permeate flow rate per hour (L/h)

A: active surface area of membrane (m^2).

As we use the same membrane throughout all the experiments, the active surface area of membrane **A** is constant and equal to 2,6 m^2.

3.3.7.4. Recovery Ratio Y

This parameter relates the amount of permeate flow to the feed flow.

If this parameter has a low value, it means that more water has been wasted and drained. But with higher values, the performance of the membrane will be worse.

Equation (4) is used to calculate the recovery ratio (Hohm, 2019), (Reverse Osmosis (RO) Fact Sheet, 2013)**.**

$$Y = \frac{Q_P}{Q_F} = \frac{Q_P}{Q_P + Q_R} \tag{4}$$

It can also be expressed as a percentage.

$$Y_{\%} = Y * 100 \tag{5}$$

Where in these equations:

Y: recovery ratio (No units)

$Y_{\%}$: recovery ratio in percentage (%)

Q_P: flow rate of permeate (L/h)

Q_R: flow rate of retentate (L/h)

Q_F: flow rate of feed (L/h)

4. Results and Discussion

4.1. Study of feed pressure influence

Feed pressure is one of the parameters that influence the most the nanofiltration process. In order to get the permeate stream flowing it must be applied to the system a minimum feed pressure, overpassing the osmotic pressure. Afterwards, the permeate flux will be increased with the pressure.

To be able to compare the feed pressure influence, it will be related in a graph with the rejection factor, calculated with the *Equation (2)*, and with the permeate flux, determined with *Equation (3)*.

In *Equation (2)* the concentration values from permeate stream and feed are calculated with the absorbances measured in the spectrophotometer and the calibration curves corresponding to each one of the dyes, as it was exposed in sections 3.3.1, 3.3.2, and 3.3.3.

Three different experiments were run with each one of the dyes, changing the feed flow in each one of them. These experiments were run in the following conditions:

- Feed pressure: from 2 to 4 bars
- Dye concentration in the feed: 50 mg/L
- pH: 7 (although it has some slight variations throughout the process)
- Feed flow: 100 L/h, 150 L/h and 200 L/h

In *Figure 4.1, Figure 4.2* and *Figure 4.3* is compared the rejection factor to the feed pressure with each one of the dyes at Q_F = 100 L/h, Q_F = 150 L/h and Q_F = 200 L/h, respectively.

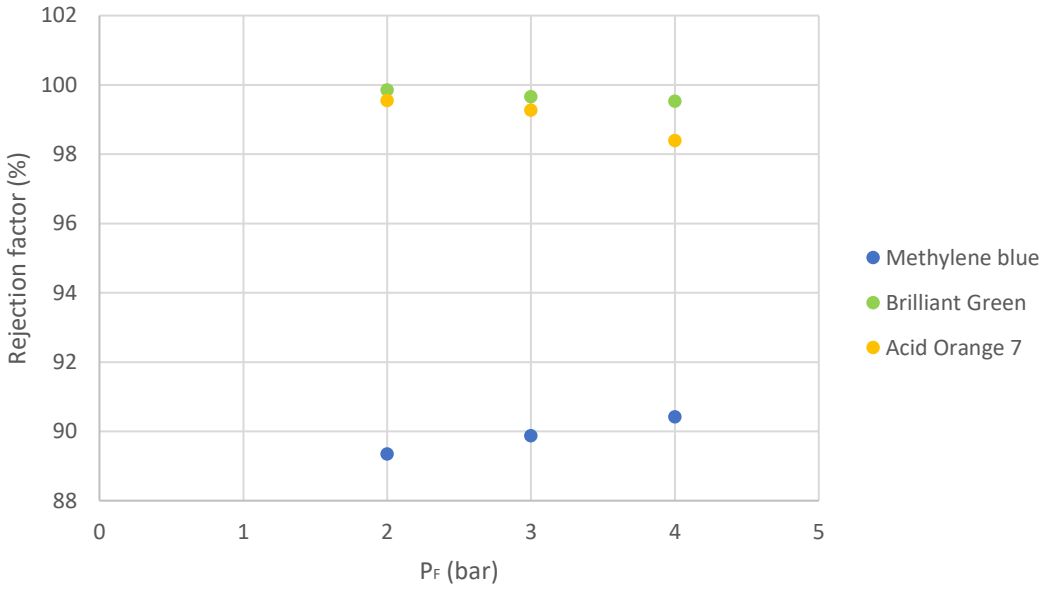

Figure 4.1. Feed pressure influence over the rejection factor at QF = 100 L/h

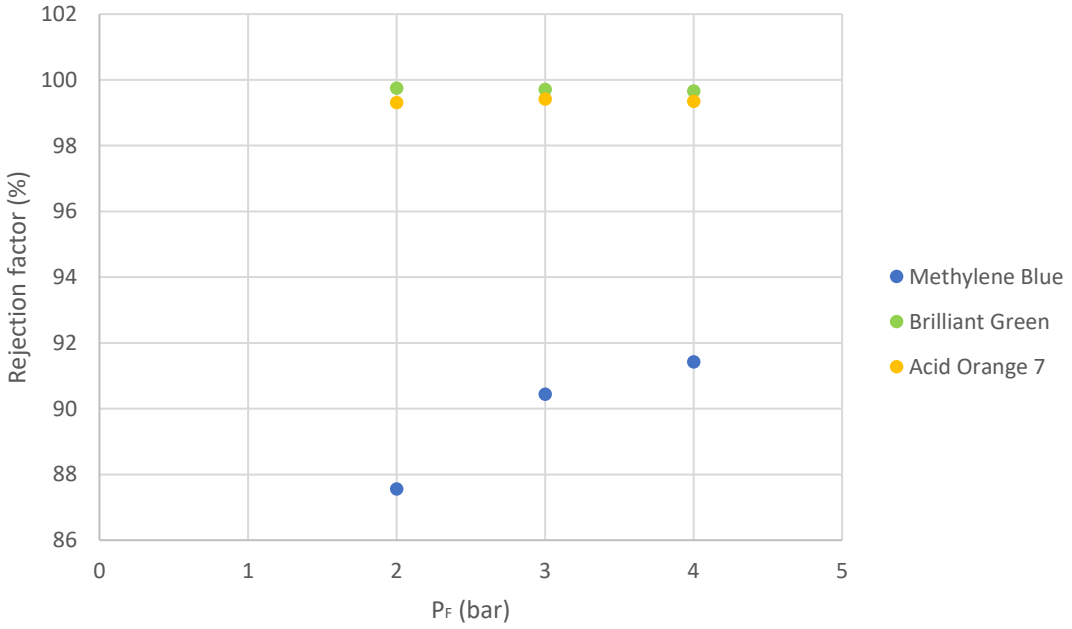

Figure 4.2. Feed pressure influence over the rejection factor at QF = 150 L/h

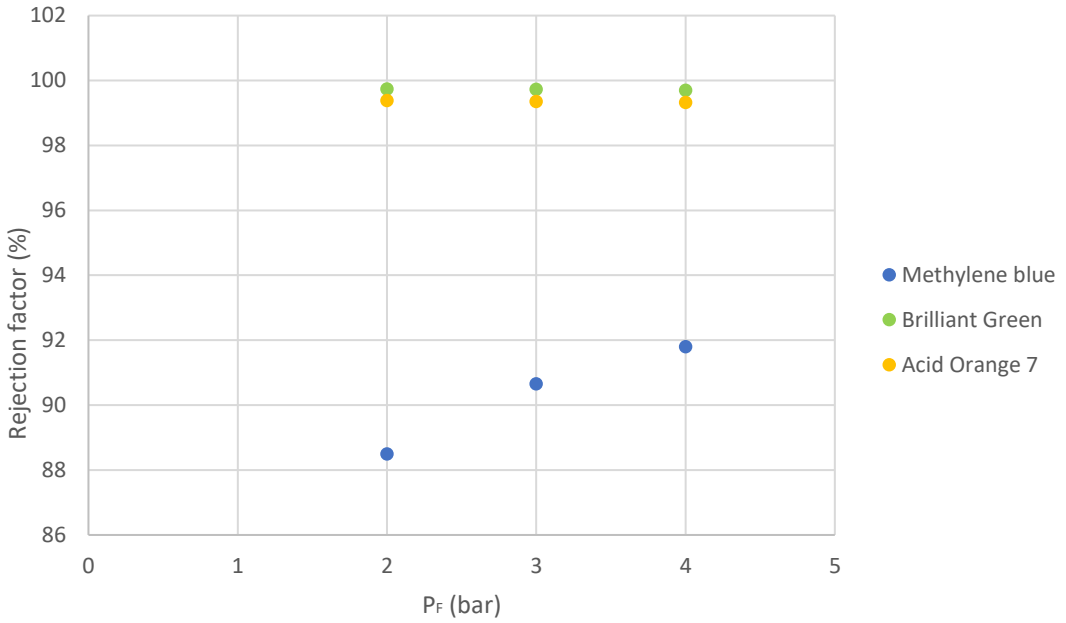

Figure 4.3. Feed pressure influence over the rejection factor at QF=200 L/h

As it can be seen on the figures above the rejection factor increases while increasing the feed pressure in the case of MB, going from a rejection factor of 89,3% to 90,4% when adjusting the feed flow to 100 L/h, from 87,6 to 91,4% when fixing the feed flow to 150 L/h, and increasing from 88,5% to 91,8% at 200 L/h, which are relatively low rejection values, maybe due to the basic character of this dye and to its low molecular weight compared to the other two dyes (319,85 g/mol), being more difficult to stop its crossing through the membrane. The increasing of the rejection factor could be because of the mechanical compaction of the membrane when operates at higher pressures. This phenomenon consists in the reduction of the volume membrane when applying a high mechanical pressure, producing a mechanical deformation of the membrane. Therefore, with this volume increasing, the pore size of the membrane decreases, which leads to a lower diffusion of the solute through the membrane, meaning higher rejection values. (Abid, Zablouk, & Abid-Alameer, 2012).

With respect to the other two dyes, in the case of BG, the rejection factor stays almost constant throughout all the process, ranging from a value of 99,8% to 99,5% at 100 L/h, which means this membrane works in a great way with this dye. Something similar happens with the AO7, but in this case the rejection factor decreases from 99,5% to 98,4% when working with a feed flow of 100 L/h, when it should increase. This may be because some factors related with the molecular characteristics (solubility, acidity, its ability to form and destroy hydrogen bonds, etc.). This kind of factors have an influence

on the solute adsorbance by the membrane and therefore, are easily transported through it, having lower rejection values. (Legaz, 2016).

In addition to the rejection factor, the feed pressure influence is also compared to the permeate flux in the *Figure 4.4, Figure 4.5* and *Figure 4.6,* adjusting the feed flow to 100 L/h, 150 L/h and 200 L/h, respectively.

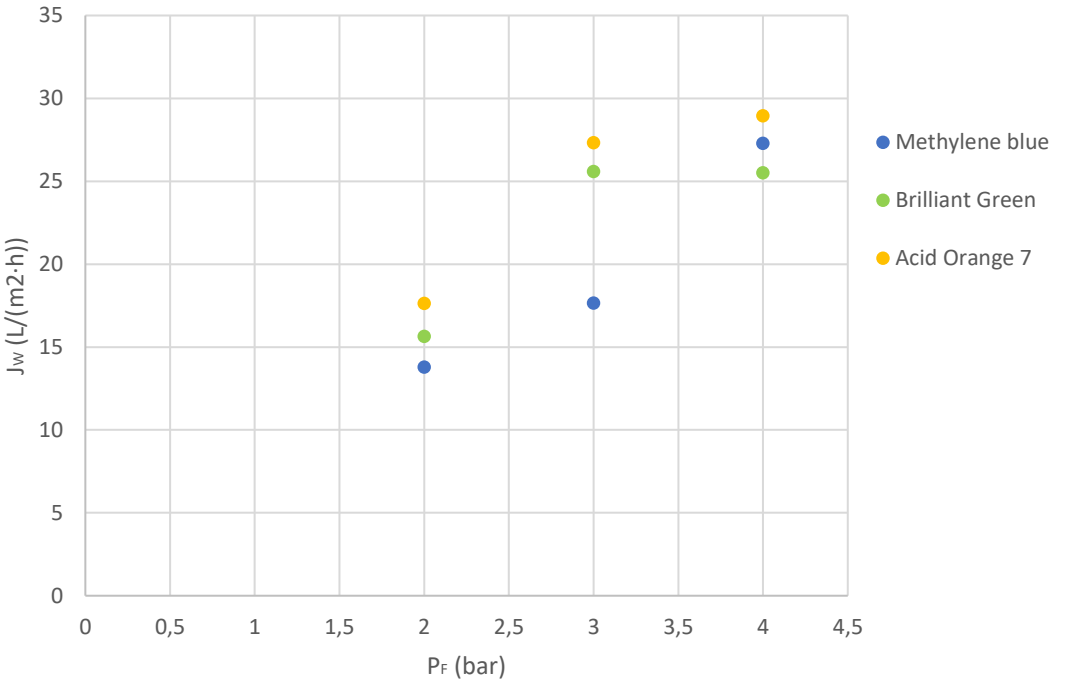

Figure 4.4. Feed pressure influence over the permeate flux at QF = 100 L/h

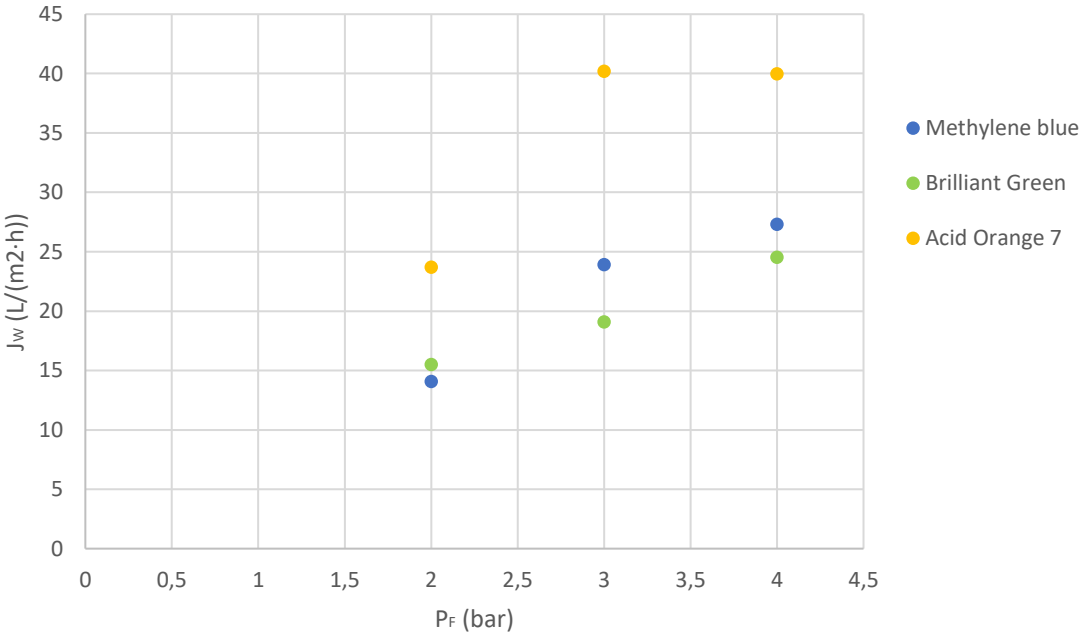

Figure 4.5. Feed pressure influence over the permeate flux at QF = 150 L/h

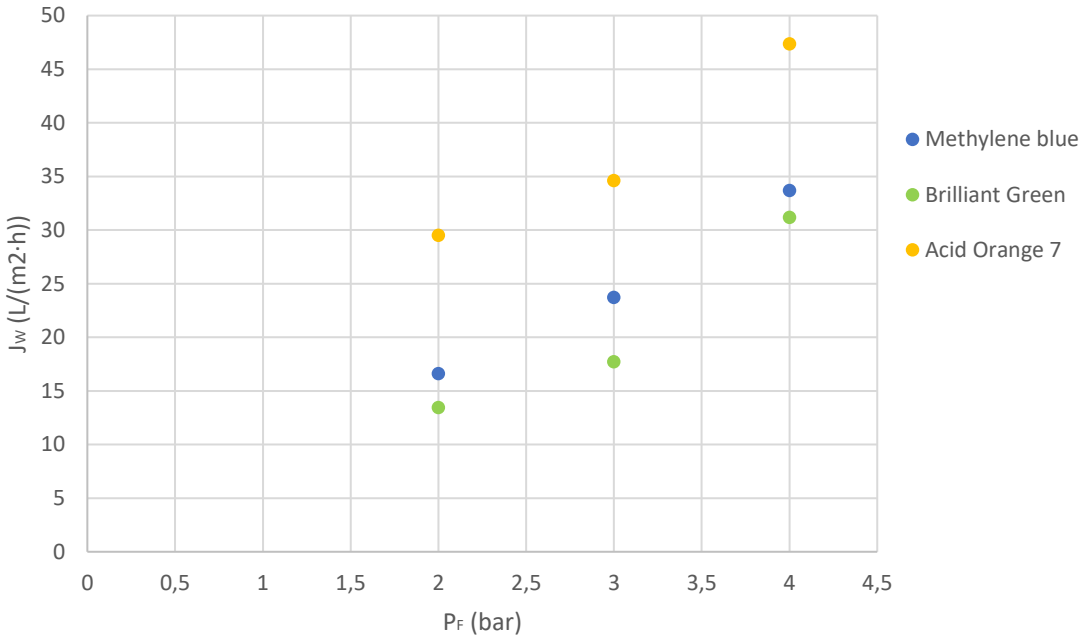

Figure 4.6. Feed pressure influence over the permeate flux at QF = 200 L/h

Observing the figures above., it can be seen that the permeate flux J_W increases with the pressure. At 4 bars, the maximum pressure, the permeate flux was the highest in the three dyes.

These results are in concordance with the fact that the driving force is increased with the rising in the feed pressure, which helps to overcome the membrane resistance.

In the *Figure 4.4* it can also be seen that, contrary with it what should be, the permeate flux in the AO7 and BG is higher than in the MB, except in the case of a feed pressure of 4 bars. Usually, the dyes with lower molecular weights are the ones with higher permeate flux, due to a smaller molecule will diffuse more quickly than a bigger molecule. (Abid, Zablouk, & Abid-Alameer, 2012). The reason for this could be the much lower solubility of the MB compared with the BG and the AO7, as it can be seen that with similar solubilities but lower molecular weight, the permeate flux of AO7 is higher than the BG.

In *Figure 4.5* and in *Figure 4.6*, the permeate flux of MB is slightly higher than the BG permeate flux, being in concordance with what was stipulated in the previous paragraph, but the permeate flux of AO7 is still way higher than the other two, probably due to its high solubility and relatively low molecular weight.

4.2. Study of feed flow influence

Feed flow has an influence on cross-flow velocity which, as seen in section 2.3.1.1., is the working principle of the nanofiltration membrane, allowing a longer operation life, preventing the accumulation of particles on the membrane surface.

In this section it will be compare in a graph the feed flow against the rejection factor, determined with *Equation (2)*, and with the permeate flux, calculated with *Equation (3)*.

As stated in the previous sections, the concentration values from both streams, permeate and feed, used in *Equation (2)* were calculated measuring the absorbances of the solutions in a spectrophotometer, as it was explained in sections *3.3.1, 3.3.2,* and *3.3.3.*

In this time again, three experiments were run with MB, BG and AO7, changing the fixed feed pressure in each one of them. These experiments were run in the following conditions:

- Feed pressure: 2,3 and 4 bars
- Dye concentration in the feed: 50 mg/L
- pH: 7 (although it has some slight variations throughout the process)
- Feed flow: from 100 L/h to 200 L/h

In Figure 4.7*, 4.8* and *4.9* is compared the rejection factor to the feed flow with each one of the dyes at A) P_F = 2 bar, B) P_F = 3 bar and C) P_F = 4 bar.

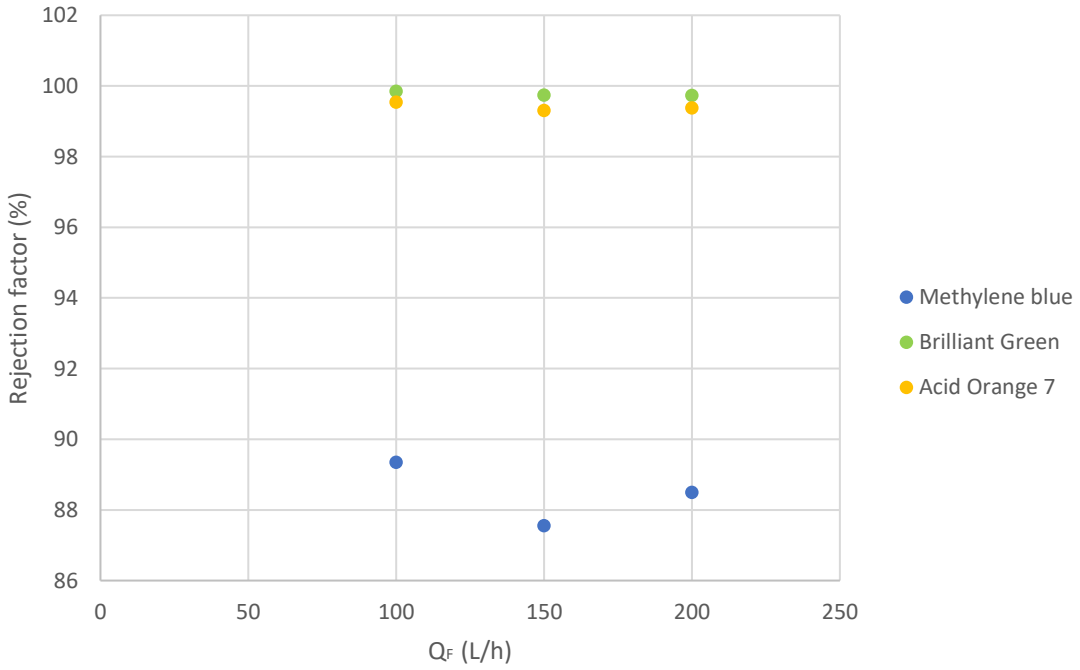

Figure 4.7. Feed flow influence over the rejection factor at PF = 2 bar

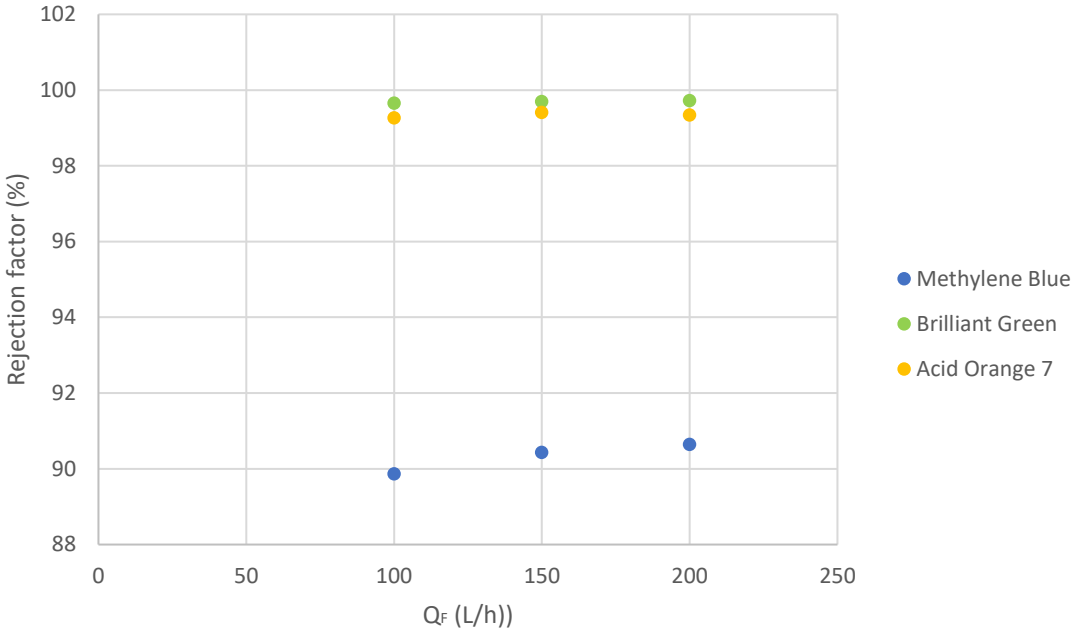

Figure 4.8. Feed flow influence over the rejection factor at PF = 3 bar

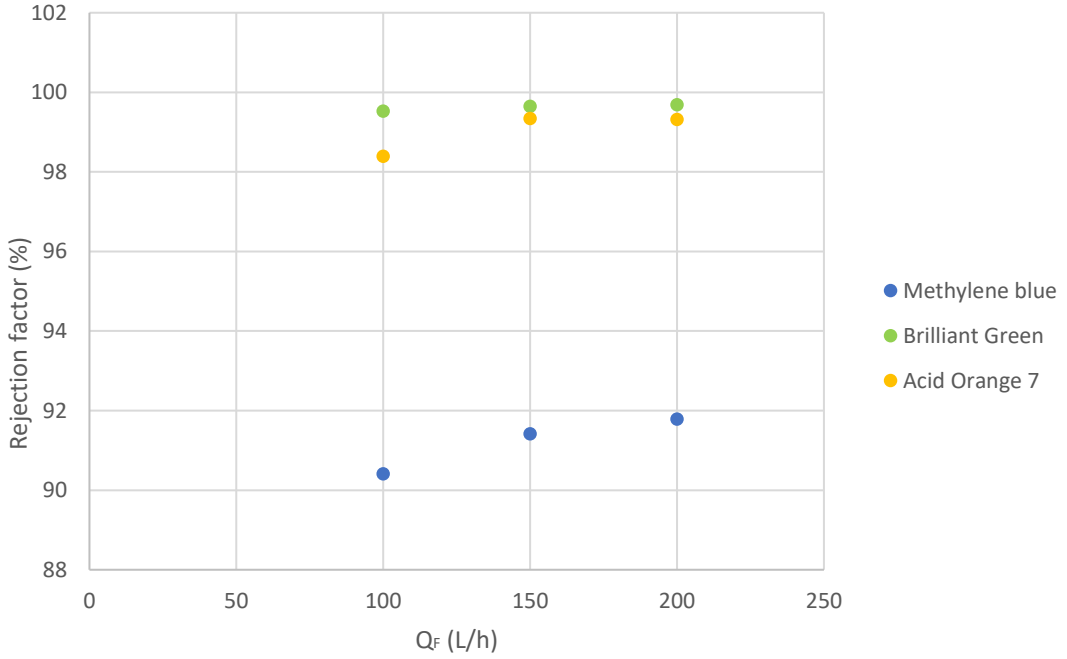

Figure 4.9. Feed flow influence over the rejection factor at PF=4 bar

In these figures it can be observed how the rejection factor increases while the feed flow is getting higher, except in the case of a feed pressure of 2 bars, where it does increase from a feed flow of 150 L/h to 200 L/h, but a slightly decrease takes place when going from 100 L/h to 150 L/h.

This is due to, as seen in section 2.3.1.2, the concentration polarization, which is directly affected by the cross-flow velocity. As the cross-flow velocity is increased, the

concentration polarization decreases, improving the membrane operation and allowing higher rejection values. (Koyuncu, 2002).

In addition to the rejection factor, the feed flow influence is also compared to the permeate flux in *Figure 4.10, Figure 4.11* and in *Figure 4.12*, adjusting the feed pressure to 2 bar, 3 bar and 4 bar respectively.

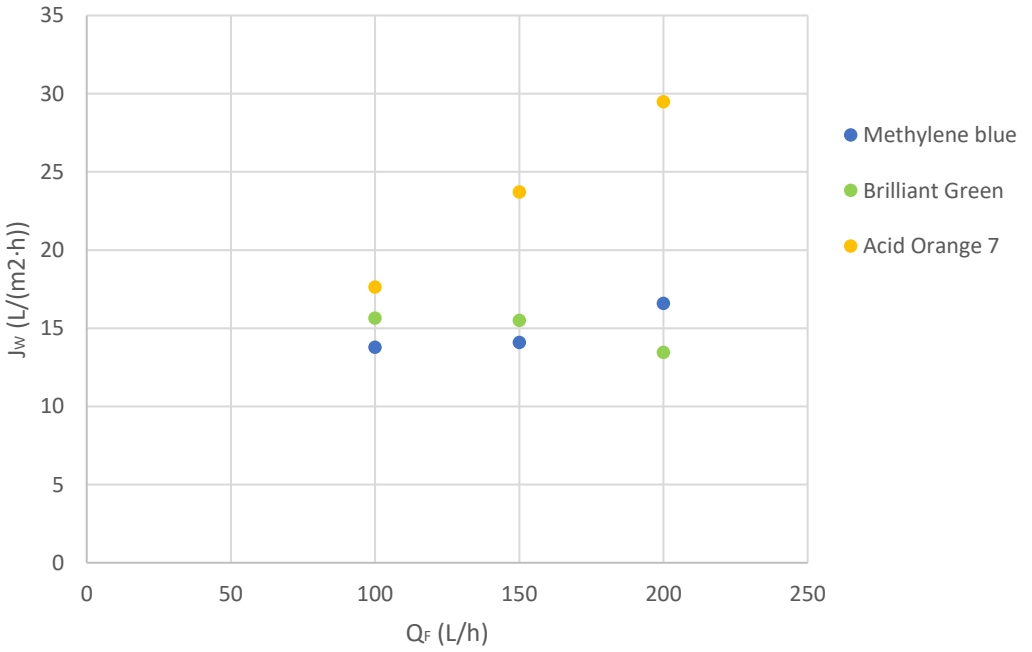

Figure 4.10. Feed flow influence over the permeate flux at PF = 2 bar

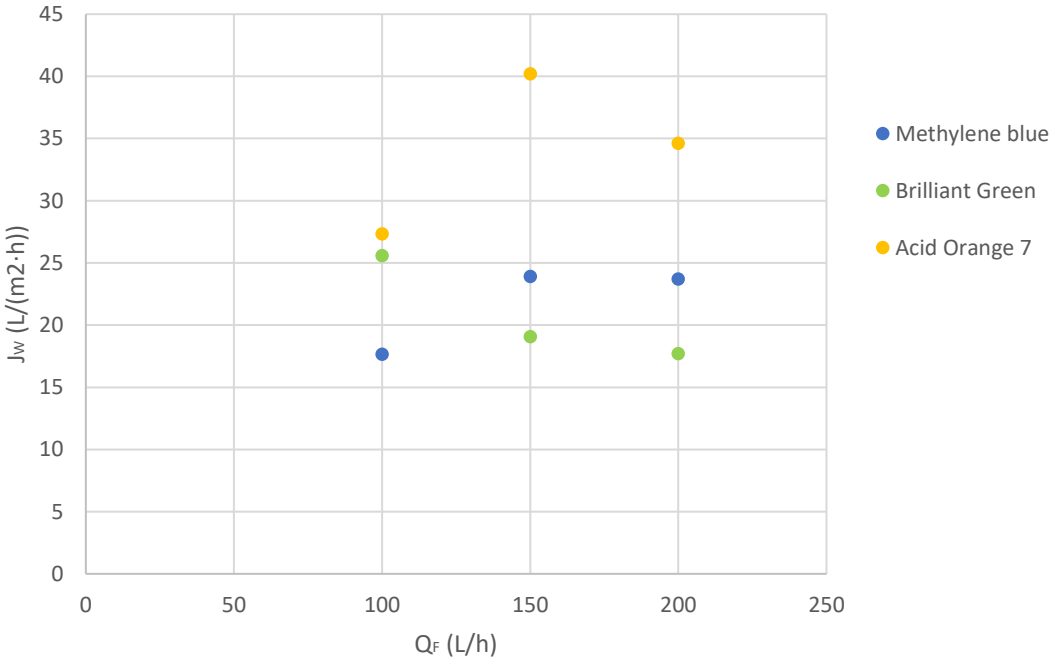

Figure 4.11. Feed flow influence over the permeate flux at PF = 3 bar

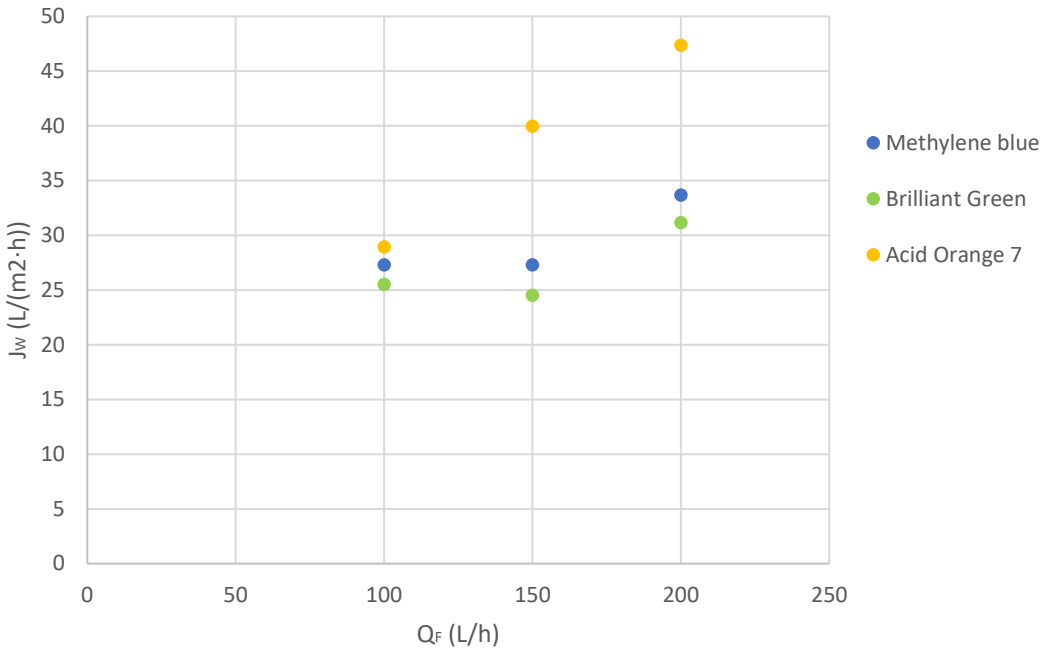

Figure 4.12. Feed flow influence over the permeate flux at PF = 4 bar

In the figures above it is generally observed how the permeate flux is increasing while the feed flow increases. The reason of this direct relation is the same as with the rejection factor: at higher feed flows, the cross-flow velocity increases, having a direct influence in the concentration polarization, making it decreasing. Once this concentration polarization is decreased, the permeate flux is optimised and is able to rise.

Nevertheless, in *Figure 4.11*, working with feed pressure at 3 bar, the increasing of this permeate flux was irregular, coming from a permeate flux of 25,6 to 17,7 (L/m2·h) in the case of BG. This situation could have its motivation in some factors such as temperature or pH changes.

As it has been seen in this section, the increasing of feed flow values optimise the membrane performance, allowing higher rejection factors and higher permeate flux. Despite this reason, the consumption of energy will be higher as we increase the feed flow, so it has to be an equilibrium between this consumption of energy and the optimisation of the membrane performance.

4.3. Study of membrane performance

In order to study the membrane performance, the recovery ratio was calculated with the *Equations (4)* and *(5)*. Comparing this value with the permeate flux allows to check if some fouling is occurring in the membrane and if some cleaning has to be performed before the membrane performance declines in a considerable way.

The feed flow was controlled with the bomb running the nanofiltration pilot plant, while the permeate flow was measured filling a little jar and stopping the time when completely filled, as it was stated in section 3.3.6.2.

Three experiments were run with MB, BG and AO7, changing the fixed feed pressure in each one of them, as well as the feed flow. These experiments were run in the following conditions:

- Feed pressure: 2,3 and 4 bars
- Dye concentration in the feed: 50 mg/L
- pH: 7 (although it has some slight variations throughout the process)
- Feed flow: from 100 L/h, 150 L/h 200 L/h

In the following figures is compared the permeate flux to the recovery ratio with each one of the dyes at P_F = 2 bar, P_F = 3 bar and P_F = 4 bar, respectively.

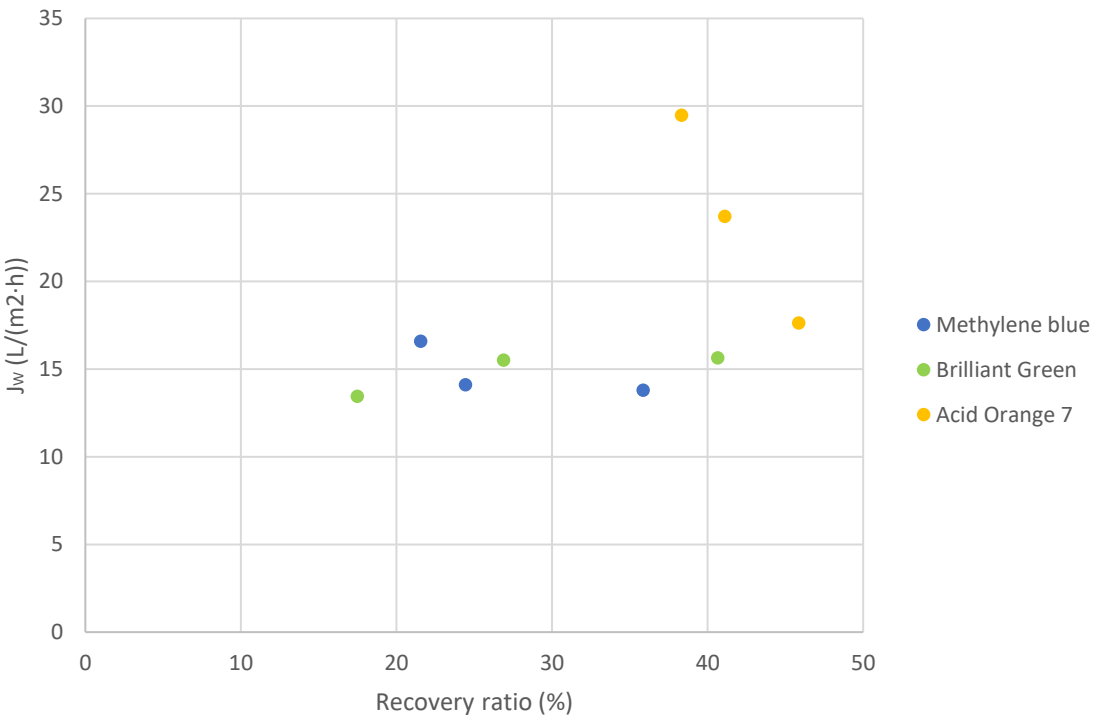

Figure 4.13. Recovery ratio relation with permeate flux at PF = 2 bar

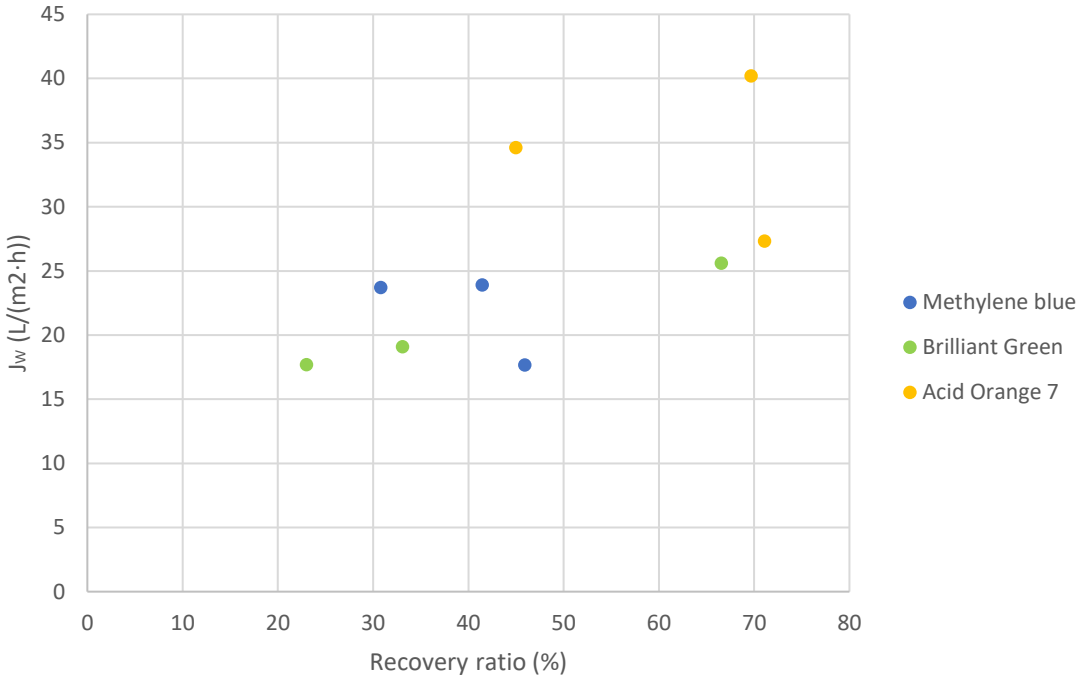

Figure 4.14. Recovery ratio relation with permeate flux at PF = 3 bar

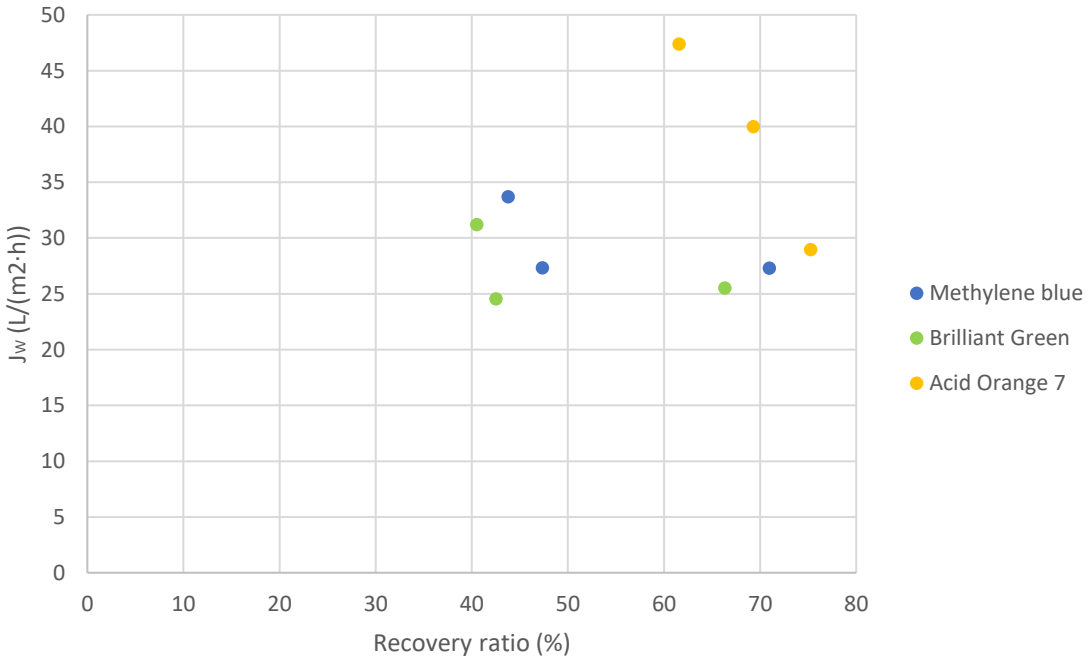

Figure 4.15. Recovery ratio relation with permeate flux at PF = 4 bar

As observed in the figures above., the relation between the recovery ratio and the permeate flux is unclear, as in the case of AO7 at 2 and 4 bars, it can be seen a decline in the permeate flux, as it is stated in the bibliography (Mendez, 2019). But in the case of MB and BG at these pressures shows a decline in some cases but not in others. This

is possibly due to the change in the operational parameters, such as the pressure itself or the feed flow, as well as slightly variances in the pH.

As stated in section 3.3.7.4, higher recovery ratio values means that the membrane performance is poor, being one of the possible reasons the concentration polarization. As this membrane was cleaned after each experiment, except when beginning the experiment with MB, this concentration polarization is not considered to be the reason of this poor membrane performance. This performance may be due to the changes in feed pressure and feed flow, along with some characteristics of the dyes, such as the solubility, acidity, etc.

If the recommended recovery ratio is exceeded, less flow goes through the membrane surface, not allowing this cross-flow to prevent the concentration polarization phenomenon. (Mendez, 2019), (Koyuncu, 2002).

In addition to the permeate flux, the recovery ratio is also compared to the rejection factor in the following figures, adjusting the feed pressure to 2 bar, 3 bar and 4 bar, respectively.

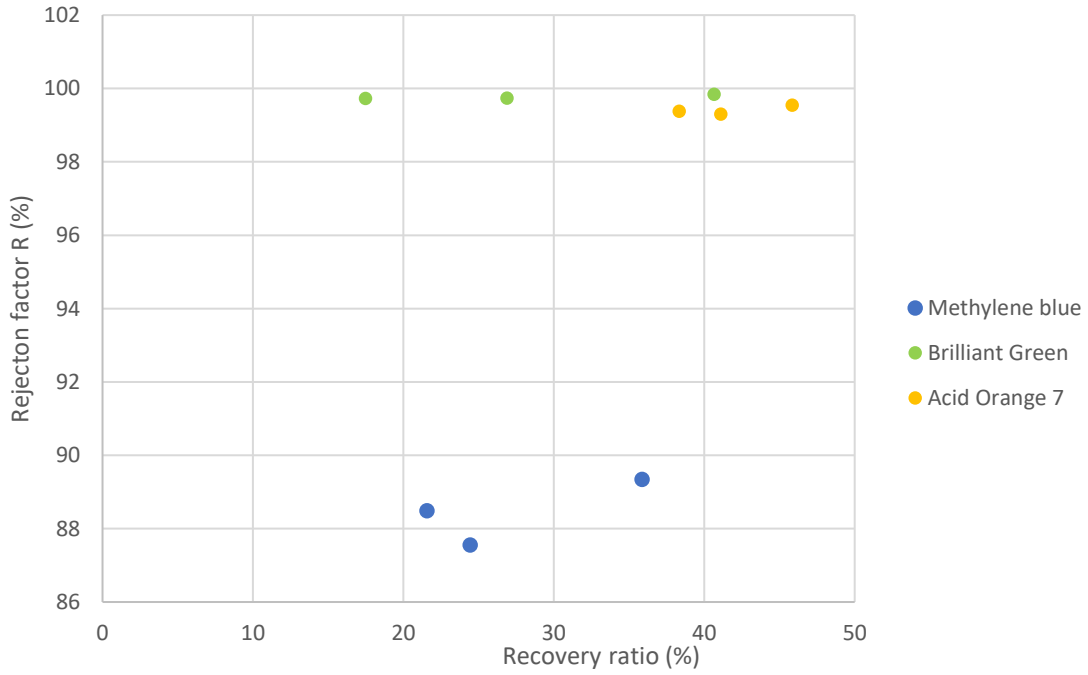

Figure 4.16. Recovery ratio relation with rejection factor at PF = 2 bar

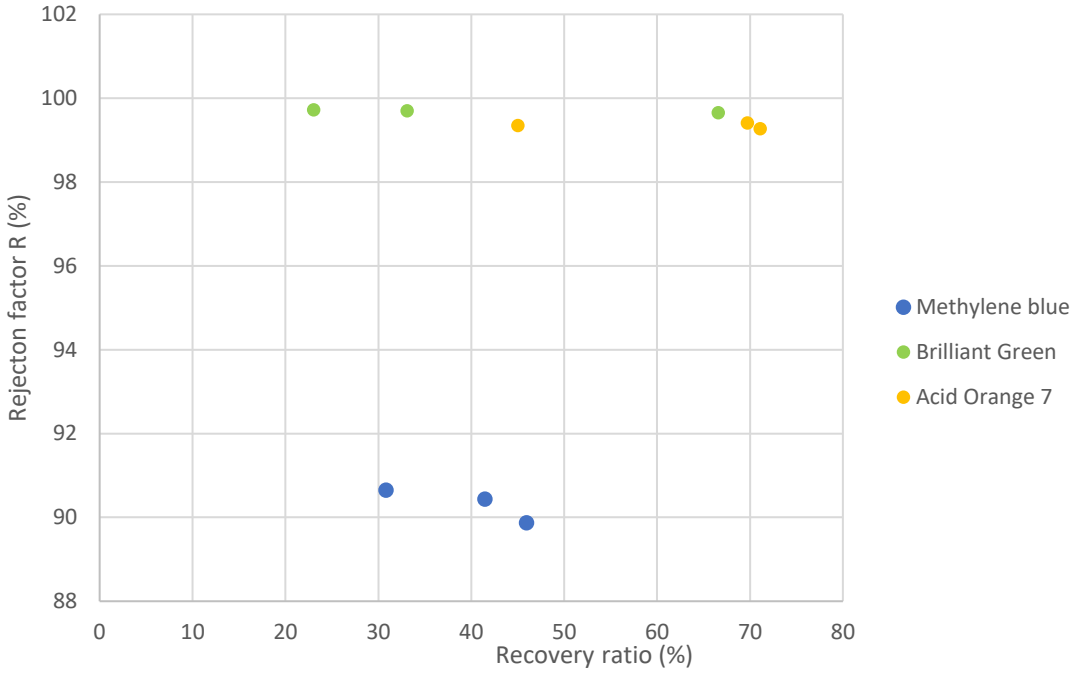

Figure 4.17. Recovery ratio relation with rejection factor at PF = 3 bar

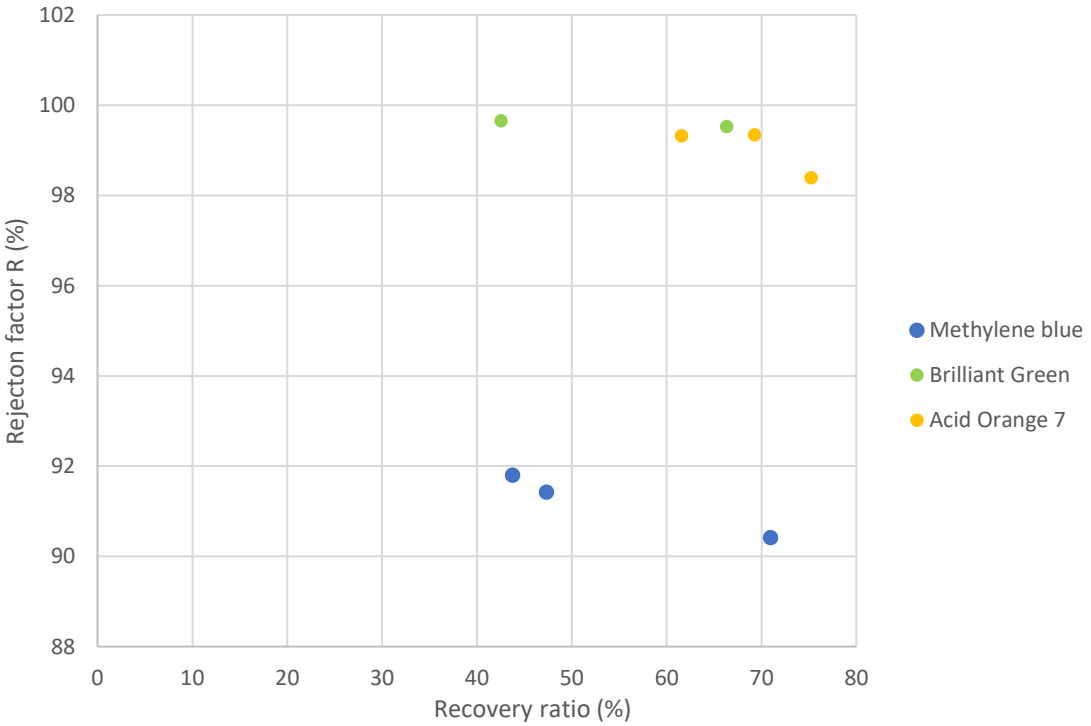

Figure 4.18. Recovery ratio relation with rejection factor at PF = 4 bar

In the case of the figures above., the relation between the recovery ratio and the rejection factor seems more clear, showing how slightly declines the rejection factor with the recovery ratio. As stated previously in this section, higher recovery ratios

translates into lower rejection factors, as lesser cross-flow is occurring on the membrane surface, allowing the appearance of the phenomenon of concentration polarization.

Nevertheless, the declining of the rejection factor values are not so high, as the highest decrease is observed in the case of the MB when working at feed pressure of 2 bar, going from a rejection factor of 91,8% with a recovery ratio of 43,8% to a 90,4% rejection factor value with a recovery ratio of 70,96%.

5. Conclusions

Once achieve the results of this work, the next conclusions could be drawn:

- The membrane shows a good rejection factor of each one of the dyes treated in these effluents, especially in the cases of BG and AO7. In the case of MB there is a good rejection factor, but it is not so high probably due to the lower molecular weight and because of its basic nature.
- When applying higher feed pressure, the rejection factor of dyes increases.
- Higher feed pressures mean higher permeate flux values.
- If the feed flow rises, the rejection factor of the dyes also increases.
- Generally, higher feed flows entail higher permeate flux.
- Energy consumption by the engine of the nanofiltration pilot plant should be considered when establishing the feed flow value, as if this feed flow is increased, the energy consumption will rise as well.
- The solubility and the molecular weight of the dye affects the rejection factor and the permeate flux.
- When studying the membrane performance, the changes in the feed flow and in the feed pressure have an influence. To make a study of which is the state of the membrane performance, these parameters should be constants, studying how the recovery ratio changes with the time.
- The recovery ratio tends to be very high, which shows a poor membrane performance in some cases despite its efficiency in eliminating the dyes. This is due to the concentration polarization phenomenon.
- Higher recovery ratios usually mean lower rejection factors.
- Higher recovery ratios usually mean lower permeate flux values.
- The chemical cleaning of the membrane is utterly important in order to make the membrane properly work when beginning each experiment and for cleaning the water from the dyes previously used in another experiments, as it happened with the first experiment with BG, where little traces of blue colour were observed in the water, due to the prior experiment with the MB. Once the chemical cleaning was done, the water was coming out of the pilot plant with no blue colour (or any other colour) at all.
- This contamination of MB was due to the lower rejection factor of the MB. When working with BG or AO7 this colour traces did not seem to appear because of its high rejection factor. Either way, the chemical cleaning was necessary.

6. References

Abid, M. F., Zablouk, M. A., & Abid-Alameer, A. M. (2012). Experimental study of dye removal from industrial wastewater by membrane technologies of reverse osmosis and nanofiltration. *Iranian journal of environmental health science & engineering, 9*, 1–9. doi:https://doi.org/10.1186/1735-2746-9-17

Ahmad, I., & Aqil, F. (2008). *New strategies combating bacterial infection.* John Wiley & Sons., ISBN: 9783527622948

Balapure, K., Bhatt, N., & Madamwar, D. (2015). Mineralization of reactive azo dyes present in simulated textile waste water using down flow microaerophilic fixed film bioreactor. *Bioresource technology, 175*, 1–7. doi:https://doi.org/10.1016/j.biortech.2014.10.040

Banerjee, P., & De, S. (2010). Steady state modeling of concentration polarization including adsorption during nanofiltration of dye solution. *Separation and purification technology, 71*, 128–135. doi:https://doi.org/10.1016/j.seppur.2009.11.012

Bashanaini, M. S., Al-Douh, M. H., & Al-Ameri, H. S. (2019). Removal of Malachite Green Dye from Aqueous Solution by Adsorption Using Modified and Unmodified Local Agriculture Waste. *Science, 7*, 42–56. doi:10.11648/j.sjac.20190702.12

Bhattacharya, D., Ghoshal, D., Mondal, D., Paul, B. K., Bose, N., Das, S., & Basu, M. (2019). Visible light driven degradation of brilliant green dye using titanium based ternary metal oxide photocatalyst. *Results in Physics, 12*, 1850–1858. doi:https://doi.org/10.1016/j.rinp.2019.01.065

Bhattacharyya, K. G., & Sarma, A. (2003). Adsorption characteristics of the dye, Brilliant Green, on Neem leaf powder. *Dyes and pigments, 57*, 211–222. doi:https://doi.org/10.1016/S0143-7208(03)00009-3

Brilliantgrün stoffdaten (2021). Obtained from https://gestis.dguv.de/data?name=490272, viewed 7 April 2021

Buscio, V., García-Jiménez, M., Vilaseca, M., López-Grimau, V., Crespi, M., & Gutiérrez-Bouzán, C. (2016). Reuse of textile dyeing effluents treated with coupled nanofiltration and electrochemical processes. *Materials, 9*, 490. doi:https://doi.org/10.3390/ma9060490

Chanikya, P., Nidheesh, P. V., Babu, D. S., Gopinath, A., & Kumar, M. S. (2021). Treatment of dyeing wastewater by combined sulfate radical based electrochemical advanced oxidation and electrocoagulation processes. *Separation and Purification Technology, 254*, 117570. doi:https://doi.org/10.1016/j.seppur.2020.117570

Damirchi, S., Maliheh, A.-K. K., Heidari, T., Es' haghi, Z., & Chamsaz, M. (2019). A comparison between digital camera and spectrophotometer for sensitive and selective kinetic determination of brilliant green in wastewaters. *Spectrochimica Acta Part A: Molecular and Biomolecular Spectroscopy, 206*, 232–239. doi:https://doi.org/10.1016/j.saa.2018.08.011

Ding, C., Yi, M., Liu, B., Han, C., Yu, X., & Wang, Y. (2020). Forward osmosis-extraction hybrid process for resource recovery from dye wastewater. *Journal of Membrane Science, 612*, 118376. doi:https://doi.org/10.1016/j.memsci.2020.118376

DOW. (s.f.). Filmtec Membranes: Product Information. Obtained from https://www.lenntech.com/Data-sheets/Dow-Filmtec-NF270-2540.pdf, viewed 14 June 2021

Elvers, B., Hawkins, S., & Schulz, G. (2002). Ullmann's encyclopedia of industrial chemistry. *Wheinhein: VCH Verlogsgesellchaft*., ISSN: 0090-7324

Geed, S. R., Samal, K., & Tagade, A. (2019). Development of adsorption-biodegradation hybrid process for removal of methylene blue from wastewater. *Journal of Environmental Chemical Engineering, 7*, 103439. doi:https://doi.org/10.1016/j.jece.2019.103439

Gholami, M., Nasseri, S., Alizadehfard, M.-R., & Mesdaghinia, A. (2003). Textile dye removal by membrane technology and biological oxidation. *Water Quality Research Journal, 38*, 379–391. doi:https://doi.org/10.2166/wqrj.2003.024

Gupta, V. K. (2009). Application of low-cost adsorbents for dye removal–a review. *Journal of environmental management, 90*, 2313–2342. doi:https://doi.org/10.1016/j.jenvman.2008.11.017

Gupta, V. K., Pathania, D., Kothiyal, N. C., & Sharma, G. (2014). Polyaniline zirconium (IV) silicophosphate nanocomposite for remediation of methylene blue dye from waste water. *Journal of Molecular Liquids, 190*, 139–145. doi:https://doi.org/10.1016/j.molliq.2013.10.027

Hadi, S., Taheri, E., Amin, M. M., Fatehizadeh, A., & Gardas, R. L. (2021). Empirical modeling and kinetic study of methylene blue removal from synthetic wastewater by activation of persulfate with heterogeneous Fenton-like process. *Journal of Molecular Liquids, 328*, 115408. doi:https://doi.org/10.1016/j.molliq.2021.115408

Hassani, A. H., Mirzayee, R., Nasseri, S., Borghei, M., Gholami, M., & Torabifar, B. (2008). Nanofiltration process on dye removal from simulated textile wastewater. *International journal of environmental science & technology, 5*, 401–408. doi:https://doi.org/10.1007/BF03326035

Heibati, B., Rodriguez-Couto, S., Turan, N. G., Ozgonenel, O., Albadarin, A. B., Asif, M., . . . Gupta, V. K. (2015). Removal of noxious dye—Acid Orange 7 from aqueous solution using natural pumice and Fe-coated pumice stone. *Journal of Industrial and Engineering Chemistry, 31*, 124–131. doi:https://doi.org/10.1016/j.jiec.2015.06.016

Hohm, B. K. (2019). *Investigation of Fouling Processes on a Nanofiltration Membrane for the Elimination of Micropollutants from the Effluent of a Municipal Treatment Plant.* Master's thesis, Hamburg University of Technology (TUHH).

Introduction to the Colour Index: Classification System and Terminology (2013). Obtained from https://colour-index.com/assets/files/upl/Introduction-to-the-Colour-Index-April-2013.pdf, viewed 3 March 2021

Kang, D., Shao, H., Chen, G., Dong, X., & Qin, S. (2021). Fabrication of highly permeable PVDF loose nanofiltration composite membranes for the effective separation of dye/salt mixtures. *Journal of Membrane Science, 621*, 118951. doi:https://doi.org/10.1016/j.memsci.2020.118951

Katheresan, V., Kansedo, J., & Lau, S. Y. (2018). Efficiency of various recent wastewater dye removal methods: A review. *Journal of environmental chemical engineering, 6*, 4676–4697. doi:https://doi.org/10.1016/j.jece.2018.06.060

Kazner, C. (2012). *Advanced wastewater treatment by nanofiltration and activated carbon for high quality water reuse.* Ph.D. dissertation, Hochschulbibliothek der Rheinisch-Westfälischen Technischen Hochschule Aachen. Obtenido de https://core.ac.uk/download/pdf/36431634.pdf

Khan, Z. U., Shah, N. S., Iqbal, J., Khan, A. U., Imran, M., Alshehri, S. M., . . . others. (2020). Biomedical and photocatalytic applications of biosynthesized silver nanoparticles: Ecotoxicology study of brilliant green dye and its mechanistic degradation pathways. *Journal of Molecular Liquids, 319*, 114114. doi:https://doi.org/10.1016/j.molliq.2020.114114

Khosravi, A., Karimi, M., Ebrahimi, H., & Fallah, N. (2020). Sequencing batch reactor/nanofiltration hybrid method for water recovery from textile wastewater contained phthalocyanine dye and anionic surfactant. *Journal of Environmental Chemical Engineering, 8*, 103701. doi:https://doi.org/10.1016/j.jece.2020.103701

Koyuncu, I. (2002). Reactive dye removal in dye/salt mixtures by nanofiltration membranes containing vinylsulphone dyes: effects of feed concentration and cross flow velocity. *Desalination, 143*, 243–253. doi:https://doi.org/10.1016/S0011-9164(02)00263-1

Legaz, J. A. (2016). *Eliminación del colorante Acid Brown-83 en efluentes líquidos mediante membranas de nanofiltración.* mathesis, Universidad de Murcia (UMU).

Li, G., Nandgaonkar, A. G., Wang, Q., Zhang, J., Krause, W. E., Wei, Q., & Lucia, L. A. (2017). Laccase-immobilized bacterial cellulose/TiO2 functionalized composite membranes: evaluation for photo-and bio-catalytic dye degradation. *Journal of membrane science, 525*, 89–98. doi:https://doi.org/10.1016/j.memsci.2016.10.033

Li, Q.-M., Ma, H.-Y., Hu, Y.-N., Guo, Y.-F., Zhu, L.-J., Zeng, Z.-X., & Wang, G. (2021). Polyamide thin-film composite membrane on polyethylene porous membrane: Fabrication, characterization and application in water treatment. *Materials Letters, 287*, 129270. doi:https://doi.org/10.1016/j.matlet.2020.129270

Luo, J., Yartym, J., & Hepel, M. (2002). Photoelectrochemical Degradation of Orange II Textile Dye on Nanostructured WO̎ 3 Film Electrodes. *Journal of New Materials for Electrochemical Systems, 5*, 315–322.

Mendez, B. L. (2019). *Micropollutant-Removal from Effluent of a Municipal Wastewater Treatment Plant by Nanofiltration with a Focus on Concentration Effects.* Master's thesis, Hamburg University of Technology (TUHH).

Orange II stoffdaten. (2021). Obtained from https://gestis.dguv.de/data?name=106453, viewed 7 April 2021

Pavithra, K. G., & Jaikumar, V. (2019). Removal of colorants from wastewater: a review on sources and treatment strategies. *Journal of Industrial and Engineering Chemistry, 75*, 1–19. doi:https://doi.org/10.1016/j.jiec.2019.02.011

PubChem. (2021). *Acid Orange 7 Compound Summary.* Obtained from https://pubchem.ncbi.nlm.nih.gov/compound/Acid-orange-7#section=Color-Additive-Status, viewed 7 April 2021

PubChem. (2021). *Brilliant Green Compound Summary.* Obtained from https://pubchem.ncbi.nlm.nih.gov/compound/Brilliant-green#section=Safety-and-Hazards, viewed 7 April 2021

PubChem. (2021). *Methylene Blue Compound Summary.* Obtained from https://pubchem.ncbi.nlm.nih.gov/compound/Methylene-blue#section=Overview, viewed 7 April 2021

Rehman, F., Sayed, M., Khan, J. A., Shah, N. S., Khan, H. M., & Dionysiou, D. D. (2018). Oxidative removal of brilliant green by UV/S2O82–, UV/HSO5–and UV/H2O2 processes in aqueous media: a comparative study. *Journal of hazardous materials, 357*, 506–514. doi:https://doi.org/10.1016/j.jhazmat.2018.06.012

Reverse Osmosis (RO) Fact Sheet. (2013) Obtained from https://www.wqa.org/Portals/0/Technical/Technical Fact Sheets/2019_RO.pdf, viewed 2 June 2021

Ricco, C., Abdmouleh, F., Riccobono, C., Guenineche, L., Martin, F., Goya-Jorge, E., . . . others. (2020). Pegylated triarylmethanes: Synthesis, antimicrobial activity, anti-proliferative behavior and in silico studies. *Bioorganic chemistry, 96*, 103591. doi:https://doi.org/10.1016/j.bioorg.2020.103591

Selvakumar, S., Manivasagan, R., & Chinnappan, K. (2013). Biodegradation and decolourization of textile dye wastewater using Ganoderma lucidum. *3 Biotech, 3*, 71–79. doi:https://doi.org/10.1007/s13205-012-0073-5

Swain, G., Singh, S., Sonwani, R. K., Singh, R. S., Jaiswal, R. P., & Rai, B. N. (2021). Removal of Acid Orange 7 dye in a packed bed bioreactor: Process optimization using response surface methodology and kinetic study. *Bioresource technology reports, 13*, 100620. doi:https://doi.org/10.1016/j.biteb.2020.100620

Technical Manual: FILMTEC Reverse Osmosis Membranes. (2016) Obtained from https://fdocuments.in/document/dow-filmtec-reverse-osmosis-technical-manual-502441510techlibfilmtecdow.html, viewed 23 March 2021

Thesnaar, L., Bezuidenhout, J. J., Petzer, A., Petzer, J. P., & Cloete, T. T. (2021). Methylene blue analogues: In vitro antimicrobial minimum inhibitory concentrations and in silico pharmacophore modelling. *European Journal of Pharmaceutical Sciences, 157*, 105603. doi:https://doi.org/10.1016/j.ejps.2020.105603

Wang, X., Xu, G., Tu, Y., Wu, D., Li, A., & Xie, X. (2021). BiOBr/PBCD-BD dual-function catalyst with oxygen vacancies for Acid Orange 7 removal: Evaluation of adsorption-photocatalysis performance and synergy mechanism. *Chemical*

Engineering Journal, 411, 128456. doi:https://doi.org/10.1016/j.cej.2021.128456

Wasewar, K. L., Singh, S., & Kansal, S. K. (2020). Process intensification of treatment of inorganic water pollutants. En *Inorganic Pollutants in Water* (págs. 245–271). Elsevier. doi:https://doi.org/10.1016/B978-0-12-818965-8.00013-5

Xiao, L., Liu, J., & Ge, J. (2021). Dynamic game in agriculture and industry cross-sectoral water pollution governance in developing countries. *Agricultural Water Management, 243*, 106417. doi:https://doi.org/10.1016/j.agwat.2020.106417

Yagub, M. T., Sen, T. K., Afroze, S., & Ang, H. M. (2014). Dye and its removal from aqueous solution by adsorption: a review. *Advances in colloid and interface science, 209*, 172–184. doi:https://doi.org/10.1016/j.cis.2014.04.002

Yukseler, H., Uzal, N., Sahinkaya, E. R., Kitis, M., Dilek, F. B., & Yetis, U. (2017). Analysis of the best available techniques for wastewaters from a denim manufacturing textile mill. *Journal of environmental management, 203*, 1118–1125. doi:https://doi.org/10.1016/j.jenvman.2017.03.041

Zuriaga-Agusti, E., Iborra-Clar, M. I., Mendoza-Roca, J. A., Tancredi, M., Alcaina-Miranda, M. I., & Iborra-Clar, A. (2010). Sequencing batch reactor technology coupled with nanofiltration for textile wastewater reclamation. *Chemical Engineering Journal, 161*, 122–128. doi:https://doi.org/10.1016/j.cej.2010.04.044

7. Appendix A

7.1. Methods

Table 7.1. Concentration (mg/L) vs Absorbance used for the calculation of Methylene Blue calibration curve.

C (mg/L)	Absorbance (λ= 665 nm)
5	0,89466222
4	0,72864
2,5	0,45156
2	0,36688
1	0,15701
0,9	0,14823
0,8	0,13761
0,75	0,12607
0,7	0,11968
0,6	0,09661
0,5	0,07610667

Table 7.2. Concentration (mg/L) vs Absorbance used for the calculation of Brilliant Green calibration curve for low concentrations.

C (mg/L)	Absorbance (λ = 624 nm)
3	0,60787
2	0,41995
1	0,21741
0,5	0,10638
0,25	0,05715
0,05	0,01451

Table 7.3. Concentration (mg/L) vs Absorbance used for the calculation of Brilliant Green calibration curve for high concentrations.

C (mg/L)	Absorbance (λ = 624 nm)
5	0,93971
4	0,7565
2	0,39605
1	0,18367
0,8	0,1444
0,6	0,10874
0,5	0,09217
0,4	0,06945
0,25	0,04169

Table 7.4. Concentration (mg/L) vs Absorbance used for the calculation of Acid Orange 7 calibration curve.

C (mg/L)	Absorbance (λ = 484 nm)
20	1,06039
18	0,95312
16	0,83427
14	0,7334
12	0,63618
10	0,52846
9	0,47738
8	0,42162
7	0,37194
6	0,31775
5	0,2642
4	0,21268
3	0,15687
2	0,10207
1	0,0488
0,75	0,03244
0,5	0,02036
0,25	0,00765

7.2. Results and Discussion

7.2.1. Methylene Blue

Table 7.5. Values of feed flow, feed pressure and concentration for the feed stream for the Methylene Blue experiment.

Q (L/h)	P_F (bar)	Conc. (mg/L)	pH
100	2	49,38126362	
100	3	48,75381264	
100	4	47,83986928	8,3
150	2	44,94281046	
150	3	48,23093682	
150	4	48,7587146	8,21
200	2	49,47875817	
200	3	49,23747277	
200	4	47,61601307	8,15

Table 7.6. Values of feed flow, feed pressure and concentration for the permeate stream for the Methylene Blue experiment.

Q (L/h)	P_F (bar)	Conc. (mg/L)	pH
100	2	5,26171024	
100	3	4,936955338	8,42
100	4	4,585784314	
150	2	5,594090414	
150	3	4,611519608	8,22
150	4	4,184095861	
200	2	5,693763617	
200	3	4,602805011	8,31
200	4	3,907271242	

Table 7.7. Values of feed flow, feed pressure and concentration for the retentate stream for the Methylene Blue experiment.

Q (L/h)	P_F (bar)	Conc. (mg/L)	pH
100	2	69,43191721	
100	3	90,67973856	8,67
100	4	131,5495643	
150	2	59,78703704	
150	3	72,82135076	8,49
150	4	95,8129085	
200	2	57,67211329	
200	3	64,11764706	8,48
200	4	76,05119826	

Table 7.8. Calculation of permeate flow when working at a certain feed pressure and feed flow for the Methylene Blue experiment

x		***P_F (bar)***		
Q_F (l/h)		2	3	4
100	m (g)	26,7024	26,2824	33,3124
	t (s)	2,68	2,06	1,69
	Qp (l/h)	**35,8688955**	**45,9304078**	**70,9613254**
150	m (g)	24,8424	29,7024	29,0024
	t (s)	2,44	1,72	1,47
	Qp (l/h)	**36,6527213**	**62,167814**	**71,0262857**
200	m (g)	24,3224	27,2224	26,7524
	t (s)	2,03	1,59	1,1
	Qp (l/h)	**43,1333202**	**61,6356226**	**87,5533091**

7.2.2. Brilliant Green

Table 7.9. Values of feed flow, feed pressure and concentration for the feed stream for the Brilliant Green experiment.

Q (L/h)	P_F (bar)	Conc. (mg/L)	pH
100	2	46,5620915	5,048
100	3	45,92374728	5,042
100	4	46,14869281	5,068
150	2	49,31862745	5,17
150	3	49,46895425	5,144
150	4	49,02178649	5,086
200	2	48,66013072	5,137
200	3	48,91013072	5,197
200	4	48,76034858	5,121

Table 7.10. Values of feed flow, feed pressure and concentration for the permeate stream for the Brilliant Green experiment.

Q (L/h)	P_F (bar)	Conc. (mg/L)	pH
100	2	0,071628533	6,335
100	3	0,158011099	6,375
100	4	0,217981818	5,934
150	2	0,126529562	6,457
150	3	0,145794383	6,248
150	4	0,169288067	6,284
200	2	0,130783156	6,216
200	3	0,133181985	6,322
200	4	0,150715692	5,89

Table 7.11. Values of feed flow, feed pressure and concentration for the retentate stream for the Brilliant Green experiment.

Q (L/h)	P_F (bar)	Conc. (mg/L)	pH
100	2	62,69880174	4,927
100	3	82,30555556	4,896
100	4	126,5250545	4,937
150	2	72,38235294	5,011
150	3	75,84858388	4,993
150	4	88,62200436	4,975
200	2	58,9422658	4,988
200	3	66,54466231	5,083
200	4	76,41884532	5,012

Table 7.12. Calculation of permeate flow when working at a certain feed pressure and feed flow for the Brilliant Green experiment.

		P_F (bar)		
Q _F (l/h)		2	3	4
100	m (g)	28,69	28,29	30,03
	t (s)	2,54	1,53	1,63
	Qp (l/h)	**40,6629921**	**66,5647059**	**66,3239264**
150	m (g)	27,67	28,13	26,05
	t (s)	2,47	2,04	1,47
	Qp (l/h)	**40,3287449**	**49,6411765**	**63,7959184**
200	m (g)	24,29	29,54	26,57
	t (s)	2,5	2,31	1,18
	Qp (l/h)	**34,9776**	**46,0363636**	**81,0610169**

7.2.3. Acid Orange 7

Table 7.13. Values of feed flow, feed pressure and concentration for the feed stream for the Acid Orange 7 experiment.

Q (L/h)	P_F (bar)	Conc. (mg/L)	pH
100	2	43,43962	6,968
100	3	49,50189	6,868
100	4	34,50189	6,987
150	2	37,03396	7,023
150	3	44,84717	6,85
150	4	46,99434	6,671
200	2	42,71132	6,911
200	3	41,30943	6,976
200	4	41,61698	6,932

Table 7.14. Values of feed flow, feed pressure and concentration for the permeate stream for the Acid Orange 7 experiment.

Q (L/h)	P_F (bar)	Conc. (mg/L)	pH
100	2	0,19802	6,756
100	3	0,36104	6,859
100	4	0,55453	6,799
150	2	0,25726	6,985

150	3	0,26274	7,014
150	4	0,30840	6,864
200	2	0,26585	6,777
200	3	0,26972	7,078
200	4	0,28377	6,802

Table 7.15. Values of feed flow, feed pressure and concentration for the retentate stream for the Acid Orange 7 experiment.

Q (L/h)	P_F (bar)	Conc. (mg/L)	pH
100	2	99,30377	6,987
100	3	171,29434	7,205
100	4	882,77358	7,5
150	2	65,45660	7,113
150	3	95,56226	7,152
150	4	141,61321	7,161
200	2	56,34717	7,268
200	3	71,72264	7,017
200	4	89,29434	7,156

Table 7.16. Calculation of permeate flow when working at a certain feed pressure and feed flow for the Acid Orange 7 experiment.

		P_F (bar)		
Q _F (l/h)		2	3	4
100	m (g)	23,82	27,84	32,82
	t (s)	1,87	1,41	1,57
	Qp (l/h)	**45,8566845**	**71,0808511**	**75,256051**
150	m (g)	24,66	29,04	28,87
	t (s)	1,44	1	1
	Qp (l/h)	**61,65**	**104,544**	**103,932**
200	m (g)	25,98	28	26,68
	t (s)	1,22	1,12	0,78
	Qp (l/h)	**76,6622951**	**90**	**123,138462**

7.3. Study of feed pressure influence

7.3.1. Rejection factor R

7.3.1.1. Methylene Blue

Table 7.17. Rejection factor calculated for different feed pressure and different feed flow

Q (L/h)	P_F (bar)	Rejection Factor (%)
100	2	89,34472337
100	3	89,87370408
100	4	90,41430426

Q (L/h)	P_F (bar)	Rejection Factor (%)
150	2	87,55286918
150	3	90,4386688
150	4	91,41877325

Q (L/h)	P_F (bar)	Rejection Factor (%)
200	2	88,49250905
200	3	90,65182522
200	4	91,79420747

7.3.1.2. Brilliant Green

Table 7.18. Rejection factor calculated for different feed pressure and different feed flow

Q (L/h)	P_F (bar)	Rejection Factor (%)
100	2	99,84616556
100	3	99,65592725
100	4	99,52765332

Q (L/h)	P_F (bar)	Rejection Factor (%)
150	2	99,74344468
150	3	99,70528105
150	4	99,65466769

Q (L/h)	P_F (bar)	Rejection Factor (%)
200	2	99,73123139
200	3	99,72770062
200	4	99,69090522

7.3.1.3. Acid Orange 7

Table 7.19. Rejection factor calculated for different feed pressure and different feed flow

Q (L/h)	P_F (bar)	Rejection Factor (%)
100	2	99,5441515
100	3	99,27065864
100	4	98,39275949

Q (L/h)	P_F (bar)	Rejection Factor (%)
150	2	99,30532912
150	3	99,41415289
150	4	99,34375878

Q (L/h)	P_F (bar)	Rejection Factor (%)
200	2	99,3775677
200	3	99,34708139
200	4	99,3181303

7.3.2. Permeate flux J_w

7.3.2.1. Methylene Blue

Table 7.20. Permeate flux calculated for different feed pressure and different feed flow

Q (L/h)	P_F (bar)	Jw (L/(m2·h)
100	2	13,795729
100	3	17,6655414
100	4	27,2928175

Q (L/h)	P_F (bar)	Jw (L/(m2·h)
150	2	14,0972005
150	3	23,9106977
150	4	27,3178022

Q (L/h)	P_F (bar)	Jw (L/(m2·h)
200	2	16,5897385
200	3	23,7060087
200	4	33,6743497

7.3.2.2. Brilliant Green

Table 7.21. Permeate flux calculated for different feed pressure and different feed flow

Q (L/h)	P_F (bar)	Jw (L/(m2·h)
100	2	15,6396124
100	3	25,60181
100	4	25,5092025

Q (L/h)	P_F (bar)	Jw (L/(m2·h)
150	2	15,5110557
150	3	19,0927602
150	4	24,5368917

Q (L/h)	P_F (bar)	Jw (L/(m2·h)
200	2	13,4529231
200	3	17,7062937
200	4	31,1773142

7.3.2.3. Acid Orange 7

Table 7.22. Permeate flux calculated for different feed pressure and different feed flow

Q (L/h)	P_F (bar)	Jw (L/(m2·h)
100	2	17,6371863
100	3	27,3387889
100	4	28,944635

Q (L/h)	P_F (bar)	Jw (L/(m2·h)
150	2	23,7115385
150	3	40,2092308
150	4	39,9738462

Q (L/h)	P_F (bar)	Jw (L/(m2·h)
200	2	29,4854981
200	3	34,6153846
200	4	47,3609467

7.4. Study of feed flow influence

7.4.1. Rejection factor R

7.4.1.1. Methylene Blue

Table 7.23. Rejection factor calculated for different feed pressure and different feed flow

P_F(bar)	Q _F (L/h)	Rejection Factor (%)
2	100	89,34472337
2	150	87,55286918
2	200	88,49250905

P_F(bar)	Q _F (L/h)	Rejection Factor (%)
3	100	89,87370408
3	150	90,4386688
3	200	90,65182522

P_F(bar)	Q _F (L/h)	Rejection Factor (%)
4	100	90,41430426
4	150	91,41877325
4	200	91,79420747

7.4.1.2. Brilliant Green

Table 7.24. Rejection factor calculated for different feed pressure and different feed flow

P_F(bar)	Q _F (L/h)	Rejection Factor (%)
2	100	99,84616556
2	150	99,74344468
2	200	99,73123139

P_F(bar)	Q _F (L/h)	Rejection Factor (%)
3	100	99,65592725
3	150	99,70528105
3	200	99,72770062

P_F(bar)	Q _F (L/h)	Rejection Factor (%)
4	100	99,52765332
4	150	99,65466769
4	200	99,69090522

7.4.1.3. Acid Orange 7

Table 7.25. Rejection factor calculated for different feed pressure and different feed flow

Q (L/h)	Q _F (L/h)	Rejection Factor (%)
100	100	99,5441515
100	150	99,30532912
100	200	99,3775677

P_F(bar)	Q _F (L/h)	Rejection Factor (%)
3	100	99,27065864
3	150	99,41415289
3	200	99,34708139

P_F(bar)	Q _F (L/h)	Rejection Factor (%)
4	100	98,39275949
4	150	99,34375878
4	200	99,3181303

7.4.2. Permeate flux J_w

7.4.2.1. Methylene Blue

Table 7.26. Permeate flux calculated for different feed pressure and different feed flow

P_F (bar)	Q _F (l/h)	Jw (L/(m2·h)
2	100	13,795729
2	150	14,0972005
2	200	16,5897385

P_F (bar)	Q _F (l/h)	Jw (L/(m2·h)
3	100	17,6655414
3	150	23,9106977
3	200	23,7060087

P_F (bar)	Q _F (l/h)	Jw (L/(m2·h)
4	100	27,2928175
4	150	27,3178022
4	200	33,6743497

7.4.2.2. Brilliant Green

Table 7.27. Permeate flux calculated for different feed pressure and different feed flow

P_F (bar)	Q _F (l/h)	Jw (L/(m2·h)
2	100	15,6396124
2	150	15,5110557
2	200	13,4529231

P_F (bar)	Q _F (l/h)	Jw (L/(m2·h)
3	100	25,60181
3	150	19,0927602
3	200	17,7062937

P_F (bar)	Q _F (l/h)	Jw (L/(m2·h)
4	100	25,5092025
4	150	24,5368917
4	200	31,1773142

7.4.2.3. Acid Orange 7

Table 7.28. Permeate flux calculated for different feed pressure and different feed flow

P_F (bar)	Q _F (l/h)	Jw (L/(m2·h)
2	100	17,6371863
2	150	23,7115385
2	200	29,4854981

P_F (bar)	Q _F (l/h)	Jw (L/(m2·h)
3	100	27,3387889
3	150	40,2092308
3	200	34,6153846

P_F (bar)	Q _F (l/h)	Jw (L/(m2·h)
4	100	28,944635
4	150	39,9738462
4	200	47,3609467

7.5. Study of membrane performance

7.5.1. Variation of recovery ratio with the rejection factor R

7.5.1.1. Methylene Blue

Table 7.29. Recovery ratio values for different feed flow pressure and feed flow related with the rejection factor

P_F(bar)	Q _F (L/h)	Rejection Factor (%)	Recovery ratio (Y)
2	100	89,34472337	35,86889552
2	150	87,55286918	24,43514754
2	200	88,49250905	21,5666601

P_F(bar)	Q _F (L/h)	Rejection Factor (%)	Recovery ratio (Y)
3	100	89,87370408	45,93040777
3	150	90,4386688	41,4452093
3	200	90,65182522	30,81781132

P_F(bar)	Q _F (L/h)	Rejection Factor (%)	Recovery ratio (Y)
4	100	90,41430426	70,96132544
4	150	91,41877325	47,35085714
4	200	91,79420747	43,77665455

7.5.1.2. Brilliant Green

Table 7.30. Recovery ratio values for different feed flow pressure and feed flow related with the rejection factor.

P_F(bar)	Q _F (L/h)	Rejection Factor (%)	Recovery ratio (Y)
2	100	99,84616556	40,66299213
2	150	99,74344468	26,88582996
2	200	99,73123139	17,4888

P_F(bar)	Q _F (L/h)	Rejection Factor (%)	Recovery ratio (Y)
3	100	99,65592725	66,56470588
3	150	99,70528105	33,09411765
3	200	99,72770062	23,01818182

P_F(bar)	Q _F (L/h)	Rejection Factor (%)	Recovery ratio (Y)
4	100	99,52765332	66,32392638
4	150	99,65466769	42,53061224
4	200	99,69090522	40,53050847

7.5.1.3. Acid Orange 7

Table 7.31. Recovery ratio values for different feed flow pressure and feed flow related with the rejection factor.

Q (L/h)	Q _F (L/h)	Rejection Factor (%)	Recovery ratio (Y)
100	100	99,5441515	45,85668449
100	150	99,30532912	41,1
100	200	99,3775677	38,33114754

P_F(bar)	Q _F (L/h)	Rejection Factor (%)	Recovery ratio (Y)
3	100	99,27065864	71,08085106
3	150	99,41415289	69,696
3	200	99,34708139	45

P_F(bar)	Q _F (L/h)	Rejection Factor (%)	Recovery ratio (Y)
4	100	98,39275949	75,25605096
4	150	99,34375878	69,288
4	200	99,3181303	61,56923077

7.5.2. Variation of recovery ratio with the permeate flux J_w

7.5.2.1. Methylene Blue

Table 7.32. Recovery ratio values for different feed flow pressure and feed flow related with the permeate flux

P_F (bar)	Q _F (l/h)	Jw (L/(m2·h)	Recovery ratio (Y)
2	100	13,795729	35,86889552
2	150	14,0972005	24,43514754
2	200	16,5897385	21,5666601

P_F (bar)	Q _F (l/h)	Jw (L/(m2·h)	Recovery ratio (Y)
3	100	17,6655414	45,93040777
3	150	23,9106977	41,4452093
3	200	23,7060087	30,81781132

P_F (bar)	Q _F (l/h)	Jw (L/(m2·h)	Recovery ratio (Y)
4	100	27,2928175	70,96132544
4	150	27,3178022	47,35085714
4	200	33,6743497	43,77665455

7.5.2.2. Brilliant Green

Table 7.33. Recovery ratio values for different feed flow pressure and feed flow related with the permeate flow

P_F (bar)	Q _F (l/h)	Jw (L/(m2·h)	Recovery ratio (Y)
2	100	15,6396124	40,66299213
2	150	15,5110557	26,88582996
2	200	13,4529231	17,4888

P_F (bar)	Q _F (l/h)	Jw (L/(m2·h)	Recovery ratio (Y)
3	100	25,60181	66,56470588
3	150	19,0927602	33,09411765
3	200	17,7062937	23,01818182

P_F (bar)	Q _F (l/h)	Jw (L/(m2·h)	Recovery ratio (Y)
4	100	25,5092025	66,32392638
4	150	24,5368917	42,53061224
4	200	31,1773142	40,53050847

7.5.2.3. Acid Orange 7

Table 7.34. Recovery ratio values for different feed flow pressure and feed flow related with the permeate flux.

P_F (bar)	Q _F (l/h)	Jw (L/(m2·h)	Recovery ratio (Y)
2	100	17,6371863	45,85668449
2	150	23,7115385	41,1
2	200	29,4854981	38,33114754

P_F (bar)	Q _F (l/h)	Jw (L/(m2·h)	Recovery ratio (Y)
3	100	27,3387889	71,08085106
3	150	40,2092308	69,696
3	200	34,6153846	45

P_F (bar)	Q _F (l/h)	Jw (L/(m2·h)	Recovery ratio (Y)
4	100	28,944635	75,25605096
4	150	39,9738462	69,288
4	200	47,3609467	61,56923077

8. Appendix B

Appendix B includes the updated and complete nanofiltration pilot plant manual

Hamburg University of Technology

Institute of Wastewater Management and Water Protection

Pilot Plant

NANOFILTRATION

User´s Manual

Institute of Wastewater Management and Water Protection B-02

Eißendorfer Str. 42 (M)
21073 Hamburg
Room 0538

Update September 2020
Version 04

Table of Contents

System and Components Description

The nanofiltration pilot plant (NFPP) is mounted on a euro-pallet and located in Technikum (Room 0358) in building M at TUHH. An overview of the process flow is shown in Figure 0-1 below.

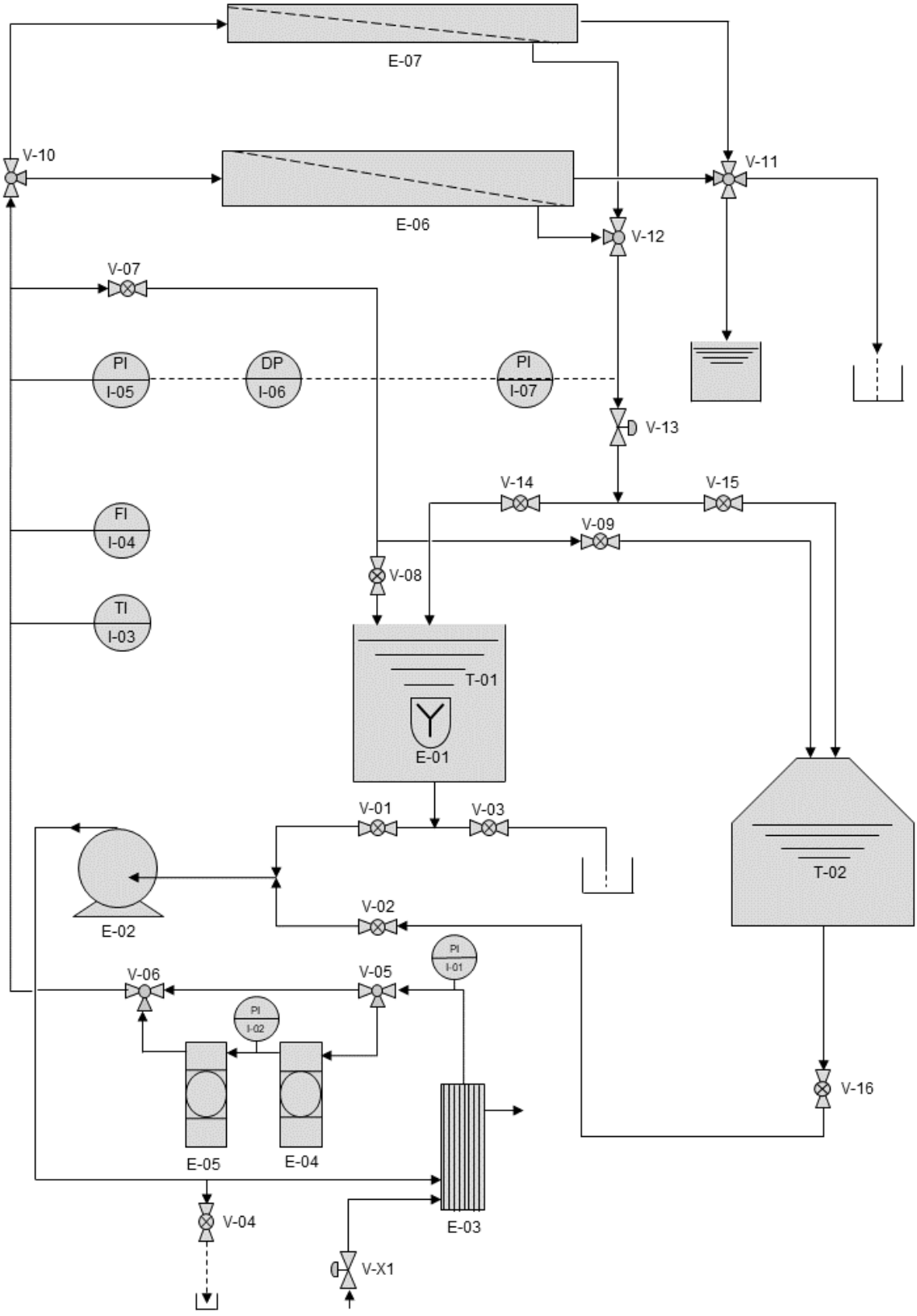

Figure 0-1 - P&ID of nanofiltration pilot plant for batch operation mode

Figure 0-2 shows images of NFPP. Equipment introduced in process flow (see Figure 0-1) as well as some additional components are identified.

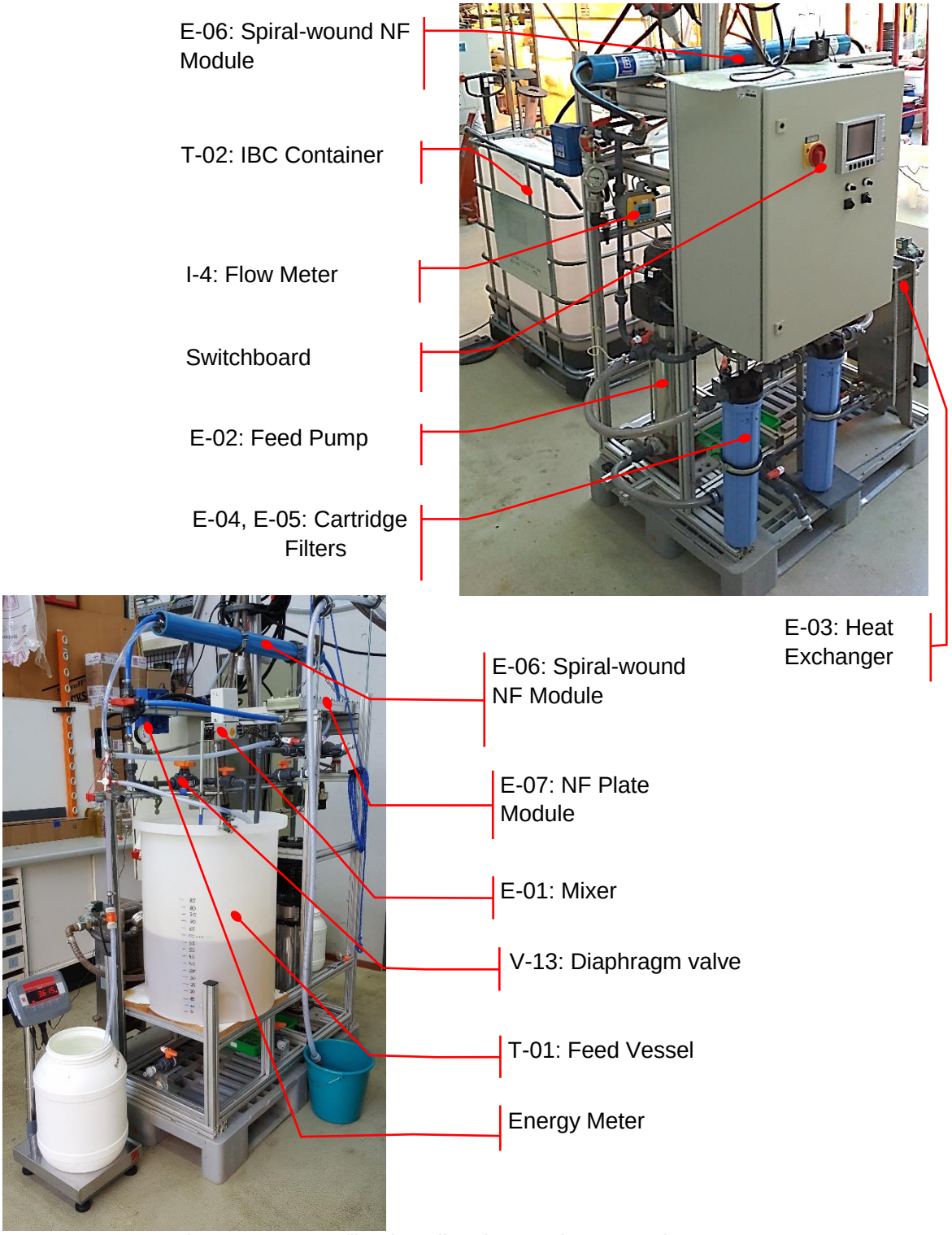

Figure 0-2 - Nanofiltration pilot plant equipment and components

Main components of system are enlisted and briefly described in Table 0-1, Table 0-2, and Table 0-3.

Table 0-1 - Equipment List

Tag	Description	Manufacturer	Material	Model
E-01	Overhead Stirrer	Heidolph	---	RZR-2000
E-02	Vertical multistage electric pump	Ebara	AISI 316 stainless steel	EVM L 3 15N5/1.5 (M)
E-03	Gasketed plate heat exchanger	GEA	Stainless steel	VT 4
E-04	Filter Housing	MTS & APIC Filter GmbH & Co.KG	Polypropylene	Big Blue AVPP 20
E-05	Filter Housing	MTS & APIC Filter GmbH & Co.KG	Polypropylene	Big Blue AVPP 20
E-06	End Port Pressure Vessel 4" 1000 psi	Phoenix	Glass reinforced epoxy resins	4E1000X.1
E-06	Nanofiltration Element Spiral-wound	Dow Chemical	Polyamide Thin-Film Composite	Filmtech NF270-2540
E-07	Nanofiltration Element Plate Modul	Variable	Variable	Variable

Table 0-2 - Instruments List

Tag	Description	Service	Manufacturer	Model
I-01	Pressure Gauge	Pressure	Wika	
I-02	Pressure Gauge	Pressure	Wika	
I-03	Temperature Transmitter	Temperature	STS Sensor Technik Sirnach AG	TS 100 290.9871.0105.30.X
I-04	Flow transmitter with integral Mount paddlewheel	Flow	G+F Signet	8512
I-05	Pressure Gauge	Pressure	IMT	
I-05	Absolute and gauge pressure	Pressure	E+H	PMS131
I-06	Differential pressure transmitter	Differential Pressure	Huba Control	692.917001
I-07	Pressure Gauge	Pressure	EMPEO	837-1
I-08	Visual Data Manager	Visualizer	E+H	Memograph RSG10-B111A21AB
I-09	Energy meters with LCD display	Energy meter	Saia-Burgess Controls	ALE3 D5F 10 Class B

Table 0-3 - Valves List

Tag	Description	Line Size	Material	Manufacturer	Model
V-01	Ball Valve 20 mm	20 mm	Industrial PVC-U	Coraplax	A-929-20
V-02	Ball Valve 20 mm	20 mm	Industrial PVC-U	Coraplax	A-929-20
V-03	Ball Valve 20 mm	20 mm	Industrial PVC-U	Coraplax	A-929-20
V-04	Ball Valve 20 mm	20 mm	PVC-U	Georg Fischer (GF)	Type 346
V-05	3-way Ball Valve 20 mm	20 mm	PVC-U / EPDM	Georg Fischer (GF)	Type 543
V-06	3-way Ball Valve 20 mm	20 mm	PVC-U / EPDM	Georg Fischer (GF)	Type 543
V-07	Ball Valve 20 mm	20 mm	PVC-U	Georg Fischer (GF)	Type 346
V-08	Ball Valve 20 mm	20 mm	PVC-U	Georg Fischer (GF)	Type 346
V-09	Ball Valve 20 mm	20 mm	PVC-U	Georg Fischer (GF)	Type 346
V-10	3-way Ball Valve 20 mm	20 mm	PVC-U	MCM Systeme (CH)	T-hole
V-11	3-way valve	10 mm	PP/PE	Bürkle	
V-12	3-way Ball Valve 20 mm	20 mm	PVC-U	MCM Systeme (CH)	T-hole
V-13	Diaphragm Valve 20 mm	20 mm	PVC-U	Coraplax	A-931-20
V-14	Ball Valve 20 mm	20 mm	Industrial PVC-U	Coraplax	A-929-20
V-15	Ball Valve 20 mm	20 mm	Industrial PVC-U	Coraplax	A-929-20
V-16	Ball Valve 20 mm	20 mm	Industrial PVC-U	Coraplax	A-929-20

The pilot plant is configured to be operated in either batch mode, recycle mode or continuous operation. For batch mode, retentate as well as permeate are selected in separate tanks and are taken out of the system. For concentration more only retentate is recycled back, while permeate is removed from the system. In continuous operation both permeate and retentate are recycled back to the feed vessel to simulate a constant incoming feed concentration. With this mode long-term experiments can be performed.

The NFPP has two feed tank alternatives, either a feed vessel (T-01) for small volumes up to 90 litres, or a larger IBC container (T-02) for up to 950 litres. It is possible to change the feed source while the pilot plant is in operation.

The feed is pumped through the system by the main feed pump (E-02). It passes a plate heat exchanger (E-03), which is supplied by the cooling circuit of Technikum, before entering pre-filters or the by-pass. The pre-filtration consists of two cartridge filters (E-04 and E-05) with two different pore sizes. Afterwards, the medium is either recirculated back to the feed vessel or flows throw the NF module (E-06/E-07).

For the nanofiltration module two different modules can be used. Either a spiral-wound NF membrane (E-06) or a plate module (E-07). The NF module are in parallel so only one can used at a time. Both retentate and permeate pipes are connected to the same outlets.

The nanofiltration module E-06 is a cylindrical pressure vessel for spiral-wound NF-membranes. The feed flows through the feed spacers. The volume permitting through membrane is collected as

permeate in the permeate tube. The retentate/ concentrate stays within the feed spacers and flows through the module to the outlet where it is collected. The functionality is visually shown in Figure 1-3.

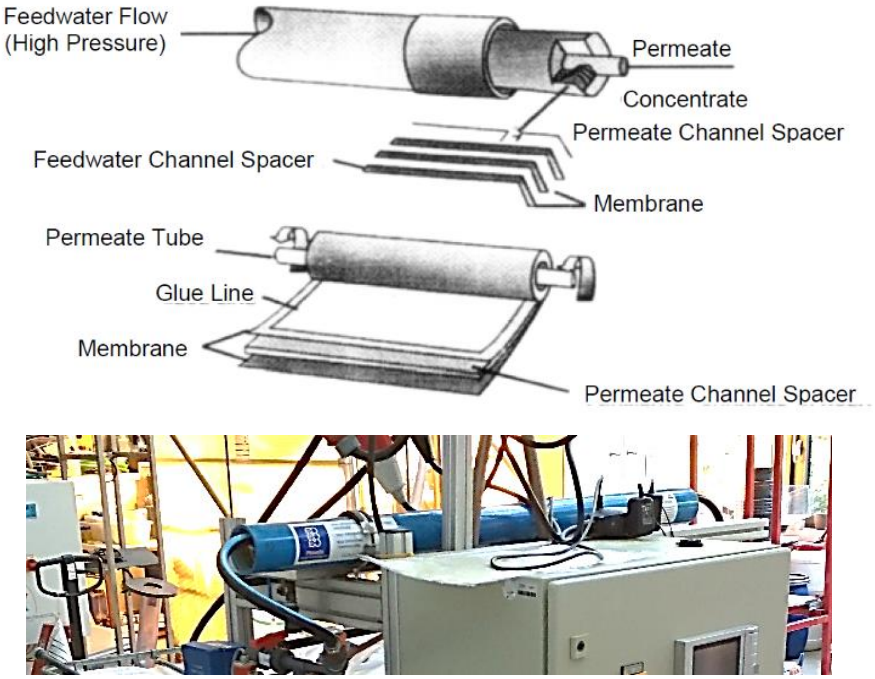

Figure 0-3 - Components of a Spiral-Wound Module (SWM) element and in parallel a picture of cylindrical pressure vessel (Dow 2018)

The nanofiltration module E-07 consists of an angular pressure vessel. One membrane sheet is placed with spacers within the pressure vessel. One feed inlet, one retentate/ concentrate outlet and two permeate outlets are given. Picture from the module are shown in Figure 1-4 below.

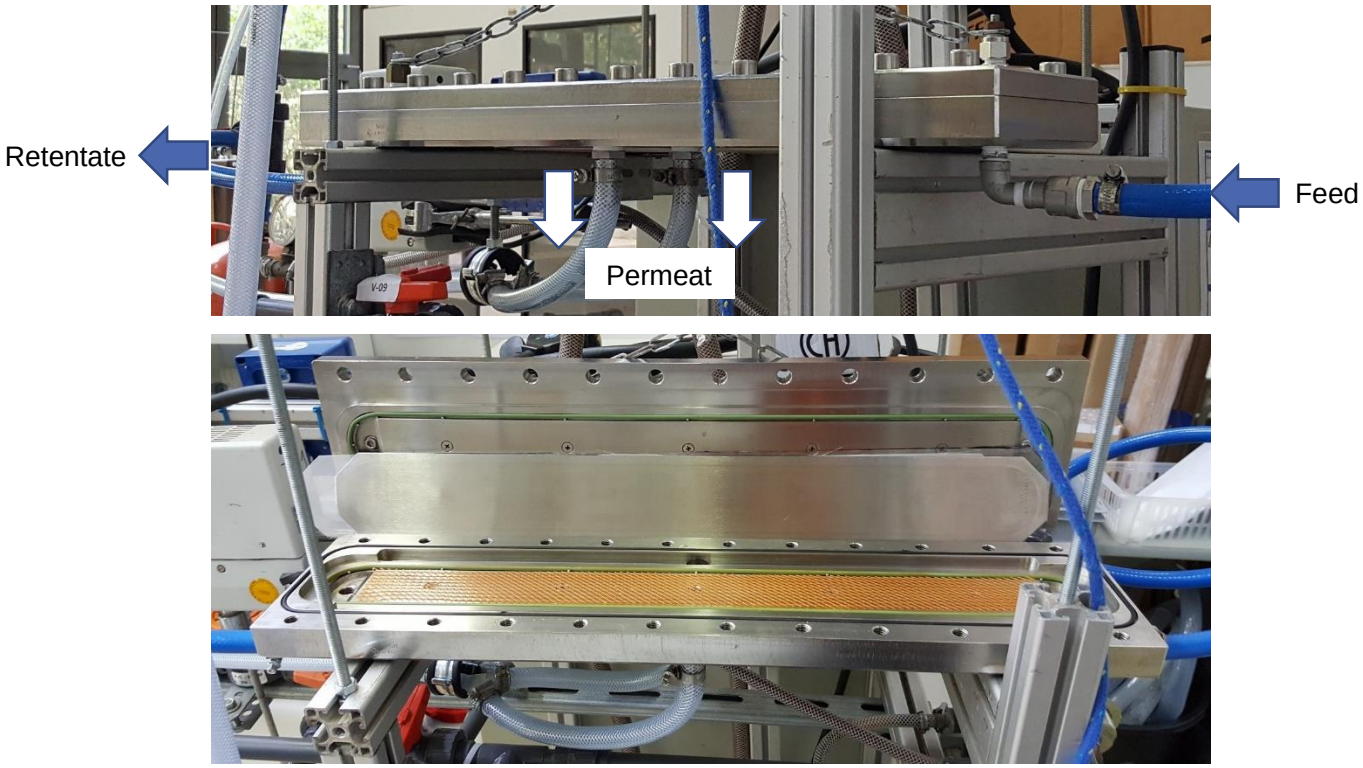

Figure 0-4 - Components of plate NF module closed and opened

Next to the experimental types batch, concentration or continuous mode, four different operational options are possible: a) recirculation (no pre-filtration and no nanofiltration), b) pre-filtration through cartridge filters, c) direct nanofiltration without pre-filtration, or d) pre-filtration and nanofiltration in line. The different operational mode set-ups are described in detail later (see Operation Modes).

At several points of the NFPP the system pressure is measured (I-01, I-02, I-05 and I-07) by pressure gauges. Also, temperature (I-03), feed flow (I-04), feed pressure (I-05), and differential pressure (I-06) between feed and retentate are measured, transmitted to the switchboard, and displayed on a screen (I-08). Data can be collected on floppy disks.

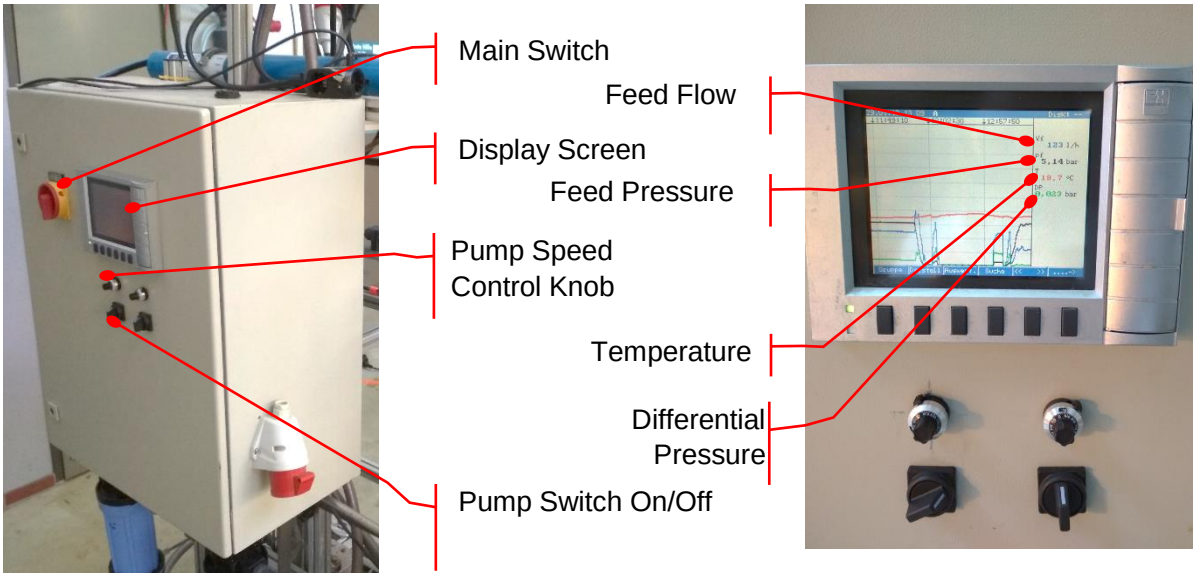

Figure 0-5 - Main switchboard components and variables displayed on screen

The switchboard supplies energy to the main feed pump (E-02) and all electronic instruments. Additional power connection is available for the feed mixer (E-01). The electric instruments have a negligible power consumption compared to the energy demand of the main feed pump. Thus, it can be assumed that the indicated power consumption on the energy meter (I-09) is proportional to the main feed pump power consumption. The instantaneous power of all phases can be checked on the energy meter (I-09) by pressing control buttons in the sequence as shown in Figure 0-6 below.

Figure 0-6 - Energy meter and control sequence to read power consumption

Operation

The following steps presume knowledge and compliance to basic safety and operation regulations stated in the operation instruction and will not be repeated in this manual. Be aware of abnormal noises or movements as well as leakages at all times.

READ THE WHOLE OPERATION SECTION BEFORE STARTING THE PLANT!

Start-Up Procedure

1. Fill the feed vessel (T-01) with the feed/ medium. Make sure valves V-01, V-02, and V-03 are closed. The vessel should be filled with at least 32 L. Thus, the water level in the feed vessel (T-01) should be equal or above the top of the main feed pump (without motor) in order to have a positive suction head.
   If you want to change the medium in the plant, you should first flush the plant with new medium in order to replace previous medium in pipes, pre-filters and the membrane. Dispose the first out coming stream (~ 10 L), refer to **Draining** procedure for further details.
   When the IBC container (T-02) is used as a feed vessel, make sure the hose is properly connected in between valves V-02 and V-16.

2. First, make sure the speed control knob and on/off switch of the feed pump (E-02) are turned all the way un-clockwise and off.
   Then, turn on the main switch on the switchboard.

3. Start cooling-liquid flow through the heat exchanger (E-3) by opening valve V-X1.

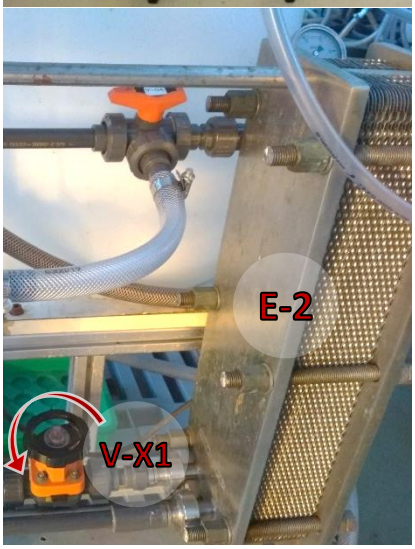

4. Make sure the speed control knob of the stirrer (E-01) is tuned at lowest speed. Plug in the stirrer and turn on the on/off switch.

5. The main feed pump (E-02) is not self-priming. If not already filled or air in the system. Use a wrench to remove the vent plug at the top of the pump body. Make sure valve V-04 is closed. Then, open valve V-01 to let the medium from feed vessel (T-01) (re-)fill the pump. When the medium starts overflowing (dropping at vent plug), screw back and tight the plug.
   Please notice that in case the medium is not reaching the top of the pump by itself, it is possible to turn on the pump and induce a small flow by raising the pump speed gradually with the speed control knob on the switchboard. As soon as water starts overflowing, turn the pump off. Then, screw back the vent plug and tight it. **AVOID ELECTRIC SHOCK!**
   A positive suction head may not always be available when using the IBC (T-02) as feed vessel. In this case, assure the pump is switched off. Then remove the vent plug completely and fill the pump by using a funnel.

6. Check the set-up of NFPP according to selected operational mode (see Table 2-1).
7. Turn on the pump switch and set the pump performance with the speed control knob.

General Operation

Once an operation mode was chosen and valves are set up as indicated in Table 2-1, continue as follows:

1. Recheck the whole system, including feed tank connections and all valves that should be opened, closed or in a specific position (three-way valves).
2. V-13 should be completely open when starting any operational mode that includes the nanofiltration.
3. Turn on the pump switch.
4. Gradually raise the pump speed with the control knob (clockwise) to regulate the pump performance. Check if water flows through the transparent hose at the pump discharge.
5. Gradually increase the flow in order to release air contained in the system.
6. Check if the set flow is following the desired path for selected operation mode. Otherwise, turn the speed of pump off, and re-check connections and valves set-up.
7. Keep raising the speed control knob (clockwise) to set the chosen feed flow.

Operation Modes

The NFPP can operate in four different modes:

- recirculation (no prefiltration and no nanofiltration)
- prefiltration through cartridge filters
- direct nanofiltration without prefiltration
- prefiltration and nanofiltration in line.

The four different operational modes can be run with either the feed vessel (T-01) or the IBC (T-02). It is also possible to change the feed source without stopping the current operation mode of the pilot plant.

But **IF YOU WANT TO CHANGE THE PROCESS OPERATION MODE TURN OFF THE PUMP INBETWEEN AND RESTART THE SYSTEM!**

For 3-way valves please see below Figure for positions mentioned in table below. Please keep in mind, that the valves can be built into the plant in different directions. Position A is always the incoming stream. Keep this in mind when checking the plant.

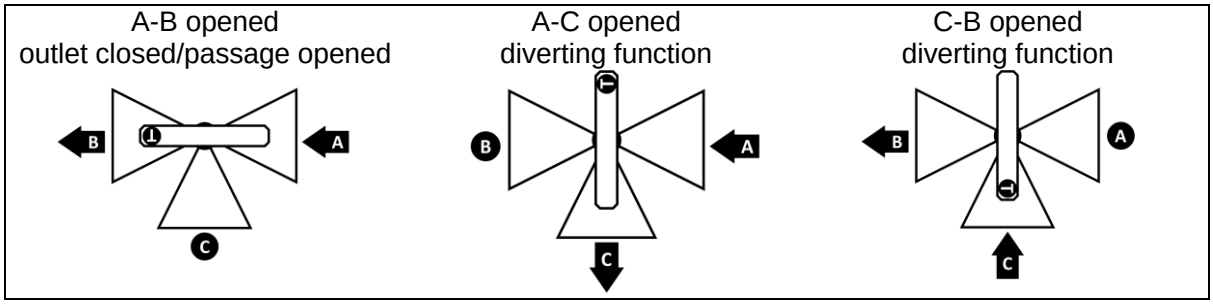

Figure 0-1 - 3-way valve positions

Table 0-1 below shows the valve set-up for the different operational modes with both feed vessels.

✗ Closed ✓ Opened AC Position

Operation Mode		V-01	V-02	V-03	V-04	V-05	V-06	V-07	V-08	V-09	V-10	V-11	V-12	V-13	V-14	V-15	V-16
Recircultion (no prefiltration and no nanofiltration)	Feed vessel (T-01).	✓	✗	✗	✗	AB	AB	✓	✓	✗	CB	CB	AC	✗	✗	✗	✗
	Feed: IBC container (T-02).	✗	✓	✗	✗	AB	AB	✓	✗	✓	CB	CB	AC	✗	✗	✗	✓
Pre-filtration Pre-filtration through cartridge filters (no nanofiltration)	Feed vessel (T-01).	✓	✗	✗	✗	AC	CB	✓	✓	✗	CB	CB	AC	✗	✗	✗	✗
	IBC container (T-02).	✗	✓	✗	✗	AC	CB	✓	✗	✓	CB	CB	AC	✗	✗	✗	✓
Direct Nanofiltration with E-06 Spiral-wound Module (no prefiltration)	Feed vessel (T-01).	✓	✗	✗	✗	AB	AB	✗	✗	✗	AC	*	AB	✓	✓	✗	✗
	IBC container (T-02).	✗	✓	✗	✗	AB	AB	✗	✗	✗	AC	*	AB	✓	✗	✓	✓
Direct Nanofiltration with E-07 Plate Module (no prefiltration)	Feed vessel (T-01).	✓	✗	✗	✗	AB	AB	✗	✗	✗	AB	*	CB	✓	✓	✗	✗
	IBC container (T-02).	✗	✓	✗	✗	AB	AB	✗	✗	✗	AB	*	CB	✓	✗	✓	✓
Pre-filtration and Nanofiltration with E-06 Spiral-wound Modul	Feed vessel (T-01).	✓	✗	✗	✗	AC	CB	✗	✗	✗	AC	*	AB	✓	✓	✗	✗
	IBC container (T-02).	✗	✓	✗	✗	AC	CB	✗	✗	✗	AC	*	AB	✓	✗	✓	✓
Pre-filtration and Nanofiltration with E-07 Plate Module	Feed vessel (T-01).	✓	✗	✗	✗	AC	CB	✗	✗	✗	AB	*	CB	✓	✓	✗	✗
	IBC container (T-02).	✗	✓	✗	✗	AC	CB	✗	✗	✗	AB	*	CB	✓	✗	✓	✓

* for this valve the position depends on batch, concentration or continuous mode. For batch mode and concentration mode valve needs to be in position AB for a collection in a separate vessel or disposing in the sink. For continuous mode it needs to be in position AC when using feed vessel (T-01) or also position AB for recycling back to IBC-Tank (T-02).

Pre-filtration Module

Pre-filtration is performed to remove particles from medium that could damage the NF module. The pre-filtration system consists of two filter housings (E-04 and E-05) each containing a 20-inch cartridge filter. Several cartridge pore sizes are available. A larger pore size cartridge is placed in E-04 and a smaller one in E-05. Usually pore sizes of 5 µm in E-04 and 1 µm in E-05 are used.

Pre-filtration can be performed beforehand or simultaneously with the nanofiltration. When feed vessel (T-01) is used, the amount of sediments left in the medium can be checked visually. A stirrer is available in the process, so sedimentation can be prevented, and pre-filtration can be performed separately before using a direct nanofiltration. In case the IBC (T-02) is used, a direct nanofiltration is not suggested, since a stirrer is not available, and sedimentation on the bottom of IBC can occur. When using the IBC (T-02) nanofiltration is only recommended to be performed simultaneously with pre-filtration

Nanofiltration Module

Figure 0-2 shows valves and equipment available at the outlet of the NF module. The retentate flow can be directed to the feed vessel (T-01) by opening V-14 and closing V-15. For a recirculation of retentate to the IBC (T-02), V-14 is closed and V-15 opened. Connect a hose to the quick coupling connector available at the outlet of V-15 to redirect the retentate stream to the IBC (T-02).

For permeate disposal V-11 is set into AB direction. Additionally, this setting can be used to recirculate permeate to the IBC (T-02) by inserting the end of the permeate pipe to the IBC instead of the sewer system. For a recirculation of permeate to the feed vessel, V-11 is set to AC.

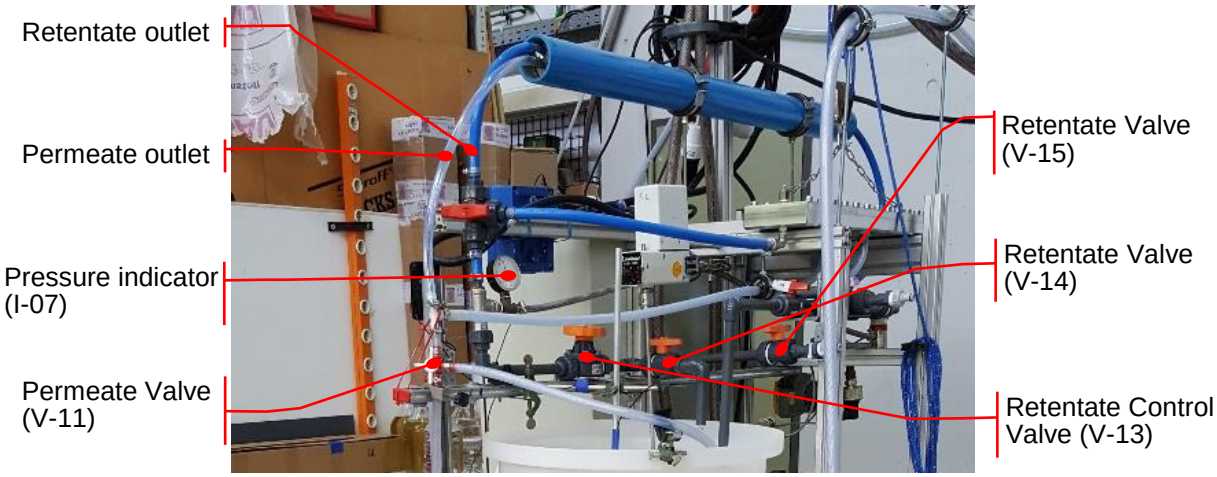

Figure 0-2 - Relevant elements in the operation of the nanofiltration module

Set flow and pressure operating point

Once **Start-Up Procedure** and General Operation steps are completed, flow rate and operation point can be set as follows:

1. Set a low feed flow (approximately 200 L/h), so membrane starts wetting (for new membranes) or replace the storage liquid. Wait for around one minute.
2. Next, gradually close (turn clockwise) the retentate control valve (V-13). This step reduces the flow and the pressure starts raising in the NF module. Move slowly as sudden pressure changes damage the NF module.
   The handwheel of diaphragm valve (V-13) can do a maximum of 3 ⅞ turns. From tests performed, an optimal control for this system (NFPP) was observed between 3 ¼ turns (≈ 85% closed) and 3 ½ turns (≈ 90% closed).
3. After an initial closing of V-13, the pressure can be further raised by increasing the pump speed with the control knob on the switchboard. To do small flow adjustments (5 - 20 L/h), turn V-13's handwheel between 1° to 5°. Close V-13 (turn clockwise) to reduce the flow and open (turn un-clockwise) to increase the flow.
   To set a selected feed flow and feed pressure, it is recommended to first raise the feed pressure by adjusting the pump speed with the control knob. Then, adjust the flow by opening or closing V-13. The speed and valve should be regulated in an iterative manner to set target feed flow and feed pressure.
   Be aware, all pressure adjustments should be done slowly to avoid damages on either pressure vessel or membrane. Remember, the feed flow and differential pressure should be continuously controlled. Both parameters are displayed on the screen of the switchboard. **THE DIFFERENTIAL PRESSURE DP SHOULD NEVER BE ABOVE 0.9 BAR!**
4. First, feed flow and pressure should be set low (approximately 200 L/h and 2 bar). Then, wait for one to two minutes, so air can be flushed out of pressure vessel or storage level is replaced.
5. Finally, set selected operation point. Raise feed pressure by controlling pump speed and adjust the flow by opening or closing V-13.

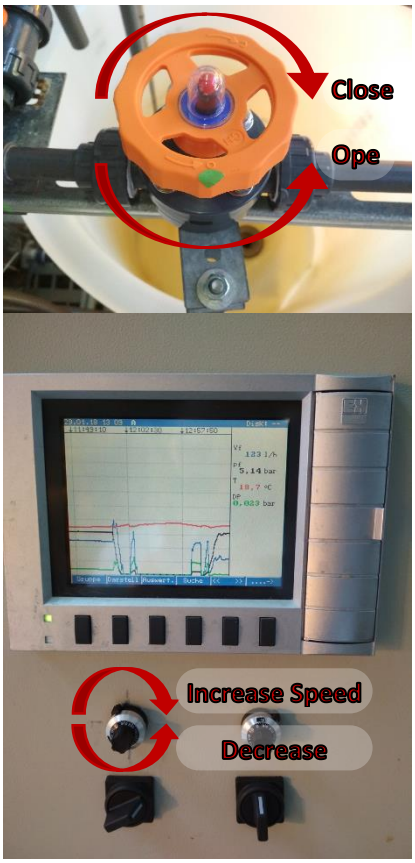

The hydraulic performance of NFPP system is influenced by the regulation of pump speed and control valve V-13. Multiple combinations of feed pressure and flow can be set by different settings pf pump speed and diaphragm valve.

Switch between feed tanks

NFPP is enabled to switch between feed tanks while running an operation mode that includes a nanofiltration. This is required to avoid damages on NF and the main feed pump (E-02) when the water level in the IBC (T-02) is below 100 L. The switch from IBC (T-02) to feed vessel (T-01) should be performed as follows:

1. The recirculated retentate flow is redirected to feed vessel (T-01). First open V-14 then slowly close V-15 to avoid a sudden raise of pressure in system.
2. Wait until feed vessel (T-1) is filled with at least 40 litres.
3. Open valve V-01, then close valve V-02.
4. Close V-16.
5. Empty the rest of IBC by using an external pump or collecting remaining feed with a jar and adding it to feed vessel (T-01).

Shutdown of nanofiltration

Start shutdown of the system by gradually reducing the pump speed (control knob un-clockwise) and opening V-13. This is performed iteratively to control the differential pressure (*DP*) ranges between 0 and 0.9 bar. *DP* is displayed on the screen of the switchboard. Please note, that the *DP* indicator cannot indicate a negative pressure difference. A negative *DP* should be avoided in order to prevent damages on NF. The diaphragm valve (V-13) should be completely open before the pump speed is set to zero. Once V-13 is opened and the pump speed is zero, turn off the pump switch and the main switch at the switch board afterwards.

When running NFPP with a medium other than tap water, the system should be drained (see section 0) and flushed (see section 0) as part of shutdown sequence. Flushing (physical cleaning) of the NFPP system is done to remove highly concentrated remainder medium in NF and the pressure vessel. This procedure must be performed before shutdown to prevent fouling. For performance loss in form of permeate flux decline or differential pressure increase, a chemical cleaning procedure must be performed additionally.

PLEASE NOTE: A MEMBRANE SHOULD NEVER BE STORED DRY IN BETWEEN EXPERIMENTS.

After draining, flushing and cleaning, deionized water or storage liquid (see manufacturers recommendations) must be introduced to the membrane for storage. The system should only be emptied/drained completely, when the membrane is changed, or while filters are replaced.

For the NFPP system run with tap water, the drain, flush and cleaning step can be skipped, but deionized water or storage liquid must be introduced into the system for a wet storage of the membrane while not being in use. For a short-time storage of a few days in between experiments tap water can also be used for storage.

Cleaning & Maintenance

The NFPP should be drained and flushed (physically cleaned) for several hours before system shut down when a medium other than tap water was in use. For tap water experiments the tap water should be replaced by deionized water or storage liquid. Follow **Start-Up Procedure** and **Shutdown of nanofiltration** for an exchange of medium.

The cleaning procedure includes a draining of the remainder medium and flushing the system with tap water as physical cleaning. For a reduction of biofouling and scaling regular chemical cleaning intervals are recommended and part of this manual. Moreover, the maintenance of pre-filtration cartridges is included.

Draining

Draining is necessary before a membrane exchange or a change of pre-filters. It is also a way to select the medium remaining in the system. Draining can be done as follows:

1. Verify that all the equipment (feed pump (E-02), stirrer (E-01), main switch on switchboard) is switched off.
2. Check valves V-01, V-02, and V-03 are closed.
3. If remainder medium is collected, place a container underneath outlet of V-03 and V-04.
4. Open valve V-03. Wait until the remainder medium contained in the feed vessel (T-01) is completely drained. Collect the last 3 litres left in the feed vessel (T-01) with help of a manual pump (see picture on the right).
5. Open valve V-01. Unscrew the vent plug at the top of feed pump (E-02) and wait until the medium contained in the pump is drained. Keep in mind, that feed pump (E-02) need to be refilled after draining of system.
6. Finally, open valve V-04 to drain the last remainder medium contained in the pipes of the NFPP system.

Flushing (Physical Cleaning)

The NFPP must be flushed before system shut down for several hours to prevent biological growth inside the NFPP system (unless it was only run with tap water). The flushing sequence is performed to ensure that highly concentrated remainder medium is removed from the NFPP system. It is also referred to as physical cleaning and proceeded as follows:

1. Connect a hose to the quick coupling connector available at outlet of V-09 and direct it to sewage drain.
2. Setup operation mode Recirculation (without nanofiltration / pre-filtration).
3. Check valves V-01 and V-03 are closed.
4. Direct the tap water hose to the feed vessel (T-01) and tight it to avoid water splashing when opening the valve of tap water supply. Usually the tap water hose is connected to a cold-water source, but also a warm-water source is available. It can easily be exchanged if required. Be aware of remaining tap water in the pipes when changing the water source. Use a bucket to collect water and prevent spilling.
5. Start filling T-01 with tap water.
6. Follow the **Start-Up Procedure**, and Fehler! Verweisquelle konnte nicht gefunden werden. procedures described in previous sections.
7. For Recirculation mode flush the system for around 2 minutes or until clean water starts coming out of the system.
8. Turn down the feed pump (E-02) speed and switch it off.
9. Set up operation mode of Pre-filtration and Nanofiltration of used NF (wither E-06 or E-07). Connect a hose to quick coupling connector available at the outlet of V-15 and direct it to the sewage drain by closing V-14 and opening V-15. Repeat steps 3 to 6.
10. Follow the **Set flow and pressure operating point** **Set flow and pressure operating point** procedure described in previous sections.
11. Flush the system for a minimum of 30 minutes. A flushing for several hours or overnight is recommended. For a flushing of several hours the tap water can be recycled into the feed vessel (T-01) after a first flush that was disposed)
12. After flushing, replace tap water by deionized water or storage liquid for a wet storage of the membrane or proceed with a chemical cleaning as shown in **Chemical Cleaning**.
13. For an exchange of medium follow **Start-Up** and **Shutdown of nanofiltration** procedures described previously.
14. Finally, check again that the main switch is turned off, tap water valve and cooling liquid valve V-X1 are closed.

Tidy up the place, wash and disinfect your hands!

Chemical Cleaning

The cleaning procedure is intended to remove fouling and scaling from the membrane. Fouling leads to a performance loss and once irreversible, cannot be removed. To prevent irreversible fouling, chemical cleaning is performed. For plate module E-07 refer to corresponding manufacturer cleaning procedure. For spiral-wound membrane NF270 (E-06), a chemical cleaning should be performed (Dow 2018, p. 122) when:

- the normalized permeate flow drops by 10 %
- the normalized differential pressure increases by 10-15 %
- the normalized salt passage increases by 5-10% (decrease in permeate quality)

It is recommended that the cleaning procedure is done at a temperature above 20°C to enhance chemical kinetics, but within pH and temperature limits enlisted in Table 0-1 (Dow 2018, p. 122):

Table 0-1 - pH range and temperature limits for chemical cleaning

Max. Cleaning Temperature	50°C	45°C	35°C	25°C
pH range	Not allowed	3 – 10	1 – 11	1 – 12

The cleaning of the nanofiltration module should be done according to the manufacturer's recommendations (Dow 2018). Experiments on NFPP showed that mostly biofouling and (carbonate) scaling were present for the performed wastewater experiments. The cleaning procedure for biofouling and scaling is shown below. For more information, as well as cleaning solutions for other fouling types refer to the manufacturer's technical manual.

1. Prepare the cleaning solutions according to Table 0-2 (Dow 2018). At least 30 L of both solutions should be prepared. The cleaning solutions can be prepared directly in the feed vessel. While preparing cleaning solutions, work according to acid and alkaline safety instructions. Mark the feed vessel with "cleaning in process" sign for laboratory safety.

Table 0-2 - Cleaning solutions for biofouling and scaling

Cleaning solutions	**Cleaning solutions wanted by manufacturer**
Biofouling	0.1 wt% NaOH (sodium hydroxide) pH 13, 35°C maximum,
Carbonate Scaling	0.2% HCl (hydrochloric acid or muriatic acid) pH1- 2, 35°C

*For biofouling a higher pH is wanted than allowed cleaning pH range, thus perform a shorter soaking or reduce concentrations to achieve a lower pH to prevent damages in the membrane when performing a long soaking. For a scaling reduction, the recommended concentration was not compatible with wanted pH, thus a smaller concentration was used with a longer soaking time.

2. Displace water remaining in the NFPP system after flushing or storage with the prepared alkaline solution (pH 12-13) to avoid a dilution of the cleaning solution. Set a feed pressure ranging 1.5 to 2 bar and a feed flow rate ranging from 350 to 600 l/h. Follow the next steps:
   a. Set up the operation mode Pre-filtration and Nanofiltration from feed vessel (T-01). Connect a hose to the quick coupling connector available at the outlet of V-15 and direct it to the sewage drain by closing V-14 and opening V-15.
   b. Follow the **Start-Up Procedure**, and Fehler! Verweisquelle konnte nicht gefunden werden. procedures described in previous sections.
   c. Follow the **Set flow and pressure operating point** procedure described in previous sections.
   d. Flush the system for around 2 minutes with the cleaning solution.
   e. Follow the **Shutdown of nanofiltration** procedure described previously.

3. Allow the nanofiltration module to soak with the cleaning solution for about 60 minutes or overnight for lower cleaning pH (alkali) or concentration (acid). Close valves V-10, V-11, and V-15. For an overnight soaking let the cleaning solution recycle on a very slow flowrate.
4. Recycle the cleaning solution for 30 minutes at a pressure range of 1.5 to 4 bar and a flow rate ranging from 700 to 1200 l/h. Follow the next steps:
   a. Setup the operation mode Pre-filtration and Nanofiltration from feed vessel (T-01). Direct the permeate outlet to the feed vessel (T-01) by setting V-11 to AC.
   b. Follow the **Start-Up Procedure**, and Fehler! Verweisquelle konnte nicht gefunden werden. procedures described in previous sections.
   c. Follow the **Set flow and pressure operating point** procedure described in previous sections.
   d. Recirculate the cleaning solution through the NFPP system for around 30 minutes.
   e. Follow the **Shutdown of nanofiltration** procedure described previously.
5. Dispose the cleaning solution. Follow the **Draining** procedure described previously.
6. Repeat steps 1 to 5 with the acidic solution (pH 1-2).
7. Flush the system extensively. Follow the **Flushing** procedure described previously.
8. Store the membrane in deionized water or storage liquid.

Cartridge Filters Maintenance

The cartridge filter manufacturer recommends a replacement of cartridges for a differential pressure exceeding 1.5 bar per cartridge (MTS & APIC Filter GmbH & Co.KG 2018). The differential pressure can be calculated via pressure indicators (PI) I-01, I-02, and I-05. For E-04: I-01 minus I-02. For E-05: I-02 minus I-05. Replace filters with the following steps. Wear gloves for your own protection as medium remains in filter housings even after the pilot plant is drained.

1. Make sure the pilot plant is drained and the main feed pump as well as the main switch are off.
2. Loose rubber lined pipe clips that fix filter housings.
3. Unscrew and remove the filter housing (blue part) from the filter head (black part). This can be done with the help of a filter or strip wrench. If an easy removal is not possible, remove the entire system. Be aware to avoid a high torque on the housing to prevent a breakage of PVC-U pipe connections. For a removal of the entire system, unscrew unions at inlet and outlet of the filter head. Place unit upside down in a press for support to unscrew housing. Be aware of spillage as water is still contained in filter housings.
4. Remove the cartridge and dispose it. Wear gloves!
5. Rinse the housing and wipe the O-ring. Lubricate the O-ring with silicone grease before putting it back.
6. Place a new filter into the filter housing. Make sure the cartridge slips into the sump at bottom of the housing.
7. Grease the screw of the filter head with silicone. Screw the filter housing to the filter head until hand tight. Make sure the cartridge slips into standpipe of filter head.
8. Re-fix rubber lined pipe clip for filter housing support.
9. Check for leakages when operating the pre-filtration system. A short performance test with tap water is recommendable.

References

Dow 2018, *Technical Manual: FILMTEC Reverse Osmosis Membranes*, Dow, viewed 12 March 2018, <https://dowac.custhelp.com/app/answers/detail/a_id/3428>.

MTS & APIC Filter GmbH & Co.KG 2018, *Filter Cartridge Type AX*, MTS & APIC Filter GmbH & Co.KG, Bad Liebenzell, viewed 15 August 2018, <https://www.mts-apic-filter.de/Datenblatt%20AX%20(engl.).pdf>.